THESIS

HISTOLOGICAL AND BEHAVIORAL CHARACTERIZATION OF A MURINE MODEL OF PARKINSON'S DISEASE USING SYSTEMIC INOCULATION WITH WESTERN EQUINE ENCEPHALITIS VIRUS

Submitted by

Samantha Monica Thomas

Department of Microbiology, Immunology, and Pathology

In partial fulfillment of the requirements

For the Degree of Master of Science

Colorado State University

Fort Collins, Colorado

Summer 2025

Master's Committee:

Advisor: Lon V. Kendall

Ronald Tjalkens
Rebekah Kading

ABSTRACT

HISTOLOGICAL AND BEHAVIORAL CHARACTERIZATION OF A MURINE MODEL OF PARKINSON'S DISEASE USING SYSTEMIC INOCULATION WITH WESTERN EQUINE ENCEPHALITIS VIRUS

Parkinson's disease (PD) is the second-most common neurodegenerative disease after Alzheimer's disease, constituting over 10 million ongoing cases in humans worldwide. Disability associated with deprecations in motor function in PD is substantial, highlighting the need for better animal models to study interventions. Although the causes of PD are largely unknown, infection with mosquito-borne alphaviruses, such as Western equine encephalitis virus (WEEV), induces symptoms in humans that closely resemble those of PD. This suggests that viral inoculation may be an appropriate model to study the disease *in vivo*. Intranasal inoculation of mice with WEEV induced dopaminergic neuronal loss in the striatum (ST) and substantia nigra pars compacta (SNpc), a key pathologic feature of PD in humans. However, significant mortality in animals results from this potent, direct impact on brain tissues. This requires adjunctive immunotherapy to improve survivability. Footpad inoculation, however, may prove to be a better model due to an indirect, gradual hematologic spread to the brain. Additionally, footpad inoculation may more closely replicate central nervous system (CNS) pathology, as it mimics the natural route of infection with this mosquito-borne virus. We hypothesize that systemic WEEV infection will induce behavioral and histopathologic changes resembling PD without requiring adjunctive immunotherapy. First, a dose escalation study was performed to evaluate the tolerability of mice to increasing doses (0.5×10^4, 1×10^4, 2×10^4, 0.5×10^5, 1×10^5, and 2×10^5 PFU) of WEEV inoculated subcutaneously into the hind footpads. Clinical observations, body

weights, bioluminescent imaging, and behavioral testing, including a pole test and a grid hang test, were performed at various time points prior to brain tissue collection to evaluate the loss of dopaminergic neurons in the ST and SNpc. It was determined that while mice displayed difficulty recovering from anesthesia associated with imaging, the highest viral dose displayed the most consistent pathologic findings. However, behavioral testing was inconsistent as it was determined that the hang test was not suitable, and the pole test needed modifications to improve grip. Finally, C57BL/6 mice were inoculated with 2×10^5 PFU of systemic WEEV to characterize the behavioral and histopathologic traits of the model fully. Observations, weights, and behavioral testing were performed at various time points before brain tissue collection at 14- and 42-days post-infection (dpi) for histopathology and plaque assays. No mortality was seen in this study, indicating that the mortality seen in the dose escalation study mice was likely related to sensitivity to anesthesia induced by systemic WEEV infection. A grip strength meter replaced the hang test, and the pole test was modified for better traction. Mice displayed significant deficiencies in both grip strength and motor coordination by 42 dpi. Plaque assays indicated increasing viral CNS titers from 14 dpi to 42 dpi. Thus, we identify key characteristics of a PD phenotype in a suitable systemic WEEV model of PD. Future studies can utilize this mouse model to investigate novel therapeutic and neurodegenerative-reducing strategies for viral Parkinsonism. This mouse model will also be used in combination with other PD risk factors, such as manganese, to create a dual-hit model to more completely recapitulate the disease process.

ACKNOWLEDGEMENTS

This thesis would not have been possible without the guidance of several individuals who contributed and extended their valuable assistance in the preparation and completion of this study in one way or another. It is a pleasure to thank those who made this thesis a possibility.

I want to thank my research supervisor, Ronald Tjalkens, for making this work possible, as well as my committee members, Ronald Tjalkens, Lonnie Kendall, and Rebekah Kading, for their invaluable feedback and guidance. I would also like to thank members of the Tjalkens lab, Tenley French, Adam Schuller, Savannah Rocha, Omar Yanouri, Megan Hager, and Aidan Briggs, for their assistance with sample processing, coordination, organization, and writing, as well as for making my time here enjoyable. I wish to thank members of the Ebel lab, Samantha Courtney and Chasity Trammel, and Phase 3 manager Susi Bennet, for their assistance in coordinating ABSL-3 procedures.

I am particularly grateful to the animal care and veterinary staff of Laboratory Animal Resources at Colorado State University for their outstanding care of the animals used in these studies. I wish to acknowledge the lives of the mice used in these studies to advance science.

Finally, I extend my appreciation to all of those in my personal life who have made this thesis possible. I wish to give special thanks to my fellow residents, classmates, and friends for their ongoing support throughout my time in the program and making this journey less daunting, as well as my family and partner for making this journey worthwhile. Last but not least, I acknowledge my canine companion, Arkose, and my feline companions, Tom and Jerry, for their cheery dispositions and plethora of cuddles. Thank you!

TABLE OF CONTENTS

LIST OF TABLES

LIST OF FIGURES

CHAPTER 1 – INTRODUCTION

The primary objective of this dissertation is to behaviorally and histologically characterize a novel mouse model of Parkinson's Disease (PD) through footpad inoculation with Western Equine Encephalitis virus (WEEV). Parkinson's disease is a progressive neurodegenerative disorder that affects over 10 million people worldwide with severely disabling motor symptoms [1]. The case incidence is increasing every year as our population ages, creating a significant and growing financial and medical burden on society [2]. In the United States alone, the estimated cost of PD is estimated to be $52 billion, not including indirect costs like caretaking [3]. Not only is this a significant economic burden, but treatment options are also limited to symptomatic relief and do nothing to modify the course of the disease. The effectiveness of these palliative drugs diminishes as the severity of clinical symptoms increases due to the progression of the underlying neurodegeneration [4]. Currently, no therapeutics are capable of preventing or slowing the progression of the disease. Thus, relevant animal models are crucial for testing interventions that can effectively enhance quality of life, reduce continued neurodegeneration, and relieve the economic burden associated with this motor disability.

PD is characterized by a loss of voluntary motor control secondary to targeted degeneration of dopaminergic neurons in the substantia nigra pars compacta (SNpc) [5]. Most cases of PD are of unknown origin, described as idiopathic or sporadic PD. Although the etiology of PD remains elusive, neuronal degeneration is associated with neuroinflammatory histopathologic changes in the central nervous system (CNS), including oxidative stress, astrocyte and glial cell activation, and α-synuclein protein aggregation [5]. Various predisposing environmental factors, including

heavy metals such as manganese and lead, toxins such as pesticides, and infectious agents, have been strongly associated with neuroinflammation and the subsequent development of PD [6].

In particular, viral encephalitis has been associated with an increased incidence of PD among human survivors [7]. Exposure of the human central nervous system (CNS) to certain viruses has been shown to induce a neuroinflammatory and, later, a neurodegenerative phenotype that mimics pathology and neurological dysfunction observed in cases of sporadic PD [6][7]. Examples of this include herpes simplex virus type-1 (HSV-1), Epstein-Barr virus, human immunodeficiency virus (HIV), hepatitis B and C viruses, and influenza [8]. The most prominent case was the 1918 H1N1 Spanish influenza outbreak, which resulted in an "encephalitis lethargica" in many of the 500 million infected people during the pandemic [9]. Close to 80% of survivors who recovered from this encephalitis lethargica developed Parkinsonian-like symptoms much later in their lives [10]. This link between viral encephalitis and the development of Parkinson's symptoms suggests that viruses may be an appropriate model for the study of PD.

WEEV and other neurovirulent alphaviruses have been shown to cause encephalitis in mouse models following aerosol, intranasal, and subcutaneous challenge. It has been previously demonstrated that intranasal infection with WEEV induced selective loss of dopaminergic neurons in the SNpc [11]. However, this method induced significant mortality in study mice that required attenuation via passive immunotherapy [12]. Peripheral infection with neuroinvasive alphaviruses can also be modeled by subcutaneous injection into the mouse footpad. We have previously shown that systemic WEEV induces viral encephalitis by hematologic spread and direct entry into the CNS through circumventricular organs (CVOs) [13]. We hypothesized that footpad inoculation of WEEV in mice would induce a parkinsonian neurological state with key histopathological and behavioral characteristics of the disease without incapacitating the study animals.

In the present study, we conducted experiments to validate a mouse model for Parkinson's disease by infecting C57BL/6 mice with McFly, a firefly luciferase-expressing recombinant variant of the McMillan of WEEV, into their hind footpads at increasing doses to determine tolerability. We evaluated their general health and neurologic functioning through various tests, including daily observations, weights, a pole test for motor coordination, and a hang test for grip strength. In addition, brain regions were subsequently evaluated for key histopathologic features of the disease, which were specific to the ST and SNpc, the targeted brain regions in PD pathology. Thus, we identify the appropriate viral dose of WEEV as 2×10^5 PFU for this novel mouse model for the study of Parkinson's disease. This viral dose was then used to fully characterize the key behavioral and histopathologic features of the model.

CHAPTER 2 – LITERATURE REVIEW

2.1 Parkinson's Disease

Parkinson's disease (PD) is a slowly progressive neurodegenerative disorder. Affecting 1 million people in the United States and 4 million people worldwide, PD is the most common movement-related disorder in the world and the second most common neurodegenerative disorder after Alzheimer's disease [1]. The economic burden of the disease is substantial, estimated at nearly $52 billion total in the United States alone in both direct medical costs and indirect costs, such as reduced employment, absenteeism, and productivity loss [3]. In addition, the projected prevalence is over 1.6 million people in the United States, with a projected total economic burden of over $79 billion by 2037 [3]. A number cannot be placed on the true burden of the disease to society, however. PD patients suffer from many debilitating effects of the illness, including serious disability requiring caretaker assistance and the risk of premature mortality.

Out of all the neurodegenerative diseases in the world, PD is the fastest growing in terms of the total number of patients and the resulting disability and deaths [14]. This is thought to be due to an aging population and an increase in exposure to environmental risk factors [15]. The number of PD cases is estimated to grow to over 12 million worldwide by 2040 [15]. These facts call for further research to reduce the disease's rising prevalence and overall societal and economic impact. In 2022, the World Health Organization (WHO) declared the need for an urgent public health response to "slow the rising incidence of PD before the burden and costs of treatments overwhelm country health services" [16]. On July 2, 2024, President Biden signed the Dr. Emmanuel Bilirakis and Honorable Jennifer Wexton National Plan to End Parkinson's Act into effect [17]. This law calls for an integrated national plan to prevent, diagnose, treat, and cure

Parkinson's and other related neurodegenerative disorders by establishing an advisory council and providing annual reports [17]. As political leaders draw more attention to the disease, research into appropriate and refined animal models becomes even more important.

2.1.1 Clinical features

In 1817, James Parkinson was the first physician to describe Parkinsonism in his classic work, "An Essay on the Shaking Palsy." [18] Among his patients, he noted not only a palsy with weakened musculature but also an involuntary tremulous motion and shaking of the limbs, clearly distinguishing the disease from others that cause palsy [18]. Parkinsonism is a syndrome characterized primarily by motor symptoms, which are common manifestations of Parkinson's disease and other neurodegenerative diseases [19]. The most common motor features of PD include bradykinesia (slowness of movement), akinesia (difficulty initiating movement), muscular rigidity and weakness, resting tremors, and postural instability [20]. These motor symptoms create a characteristic gait among PD patients, which involves short shuffling steps, but can also manifest as a marked hastening of footsteps while walking or an abrupt cessation of walking [20]. These gait disturbances result in an exacerbation of balance impairment and an increased risk of injury due to falls [21]. Prospective studies have estimated that 48-68% of people with PD will fall each year, with the incidence of hip fracture four times that of people of the same age without PD [21][22][23]. In an aging population, somatomotor symptoms create disability and injury that negatively impact quality of life.

Although PD is a disease of the CNS causing characteristic motor symptoms, there are implications for the enteric nervous system via the vagus nerve. Despite early clinical reports and neuropathological findings of gastrointestinal involvement in PD [24][25][26], it was not until the late 1980s and early 1990s that clinical neurologists fully recognized the connection [27][28]. In

addition to motor symptoms, persons with PD also suffer from a range of gastrointestinal tract (GIT) symptoms such as dysphagia, bloating, nausea, vomiting, gastroparesis, and constipation, throughout the disease course, which negatively impact their quality of life [29][30]. The pathology of the disease on the enteric nervous system creates pharyngeal discoordination, esophageal and gastric motility impairment, altered intestinal permeability, and autonomic dysfunction of the colon [31]. Severe complications requiring hospitalization may arise, including chronic pain, insufficient drug absorption, malnutrition, dehydration, aspiration pneumonia, intestinal obstruction, and megacolon [31]. In addition, there is evidence suggesting that these symptoms can precede somatomotor symptoms by up to 20 years [32][33], indicating a strong connection between GIT dysfunction and PD and the possibility of an early diagnostic indicator. Overall, the influence of CNS disease on the GIT in PD patients should not be discounted.

Finally, psychiatric manifestations of the disease should also be considered highly significant. Over half of PD patients suffer from at least one mental or emotional symptom, including depression, anxiety, hallucinations, delusions, apathy and anhedonia, impulsive and compulsive behaviors, and cognitive dysfunction, which also interfere with their quality of life [34]. Although the pathophysiology of each symptom may vary, changes in the functioning of the dopaminergic, noradrenergic, and serotonergic systems are largely to blame [35]. These symptoms contribute to an increased prevalence of suicidal ideation in PD patients, which is approximately 17-30%, two times higher than the general population [36][37]. Whether a direct cause of PD brain pathology or secondary to disability and loss of autonomy, psychiatric manifestations also decrease quality of life in PD patients.

In conclusion, the clinical features of PD diverge from purely somatomotor symptoms to encompass GIT and psychiatric manifestations as well. Symptoms that were previously regarded

as benign or clinically insignificant have more recently been included in a spectrum of severity by medical professionals. This expansion of symptoms emphasizes the need for research models to reduce these symptoms and improve quality of life.

2.1.2 Risk factors

Although the direct cause of Parkinson's disease is largely regarded as unknown, the development of PD seems to involve a complex interplay of both environmental and genetic risk factors. While the majority of PD cases are not hereditary, genetics can play a role in the development of PD [38]. There are 6 total heritable genes that are known to cause PD when mutated. In the autosomal-dominant form of PD, mutations in *SNCA (PARK1=4*) and *LRRK2* (*PARK8*) are responsible [38]. In the autosomal-recessive form of inheritance, mutations in *Parkin* (*Park2*), *PINK1* (*PARK6*), *DJ-1* (*PARK7*), and *ATP12A2* (*PARK9*) are responsible [38].

The majority of PD cases are considered sporadic or idiopathic. Epidemiologic studies suggest that less than 10% of PD patients have a family history of the disease [39]. A large genomic study in the 1990s comparing concordance rates in monozygotic and dizygotic twins estimated the heritability of PD to be less than 30% [40]. Therefore, environmental risk factors may play a larger role in the development of PD compared to genetic causes.

Exposure to metals such as lead and manganese, pesticides like rotenone and paraquat, wildlife smoke inhalation, traumatic brain injuries, and neurotropic viruses throughout life has been demonstrated to increase the risk of developing PD later in life [41][42][43][44][7]. This is likely why rural farm workers and miners are among the highest-risk occupational groups [45][46]. To add to the complexity of this disease, the development of pathology is likely multifactorial, involving repeated exposures to multiple environmental risk factors throughout a person's life,

which can drastically differ from case to case [47]. At the same time, exposure to certain risk factors such as wildfire smoke, once thought to affect firefighters primarily, is increasing globally. Population exposure to fine particulate matter primarily from wildfire smoke is expected to increase based on projected wildfire trends in the United States [48]. Although we can do our best to reduce exposure to heavy metals, pesticides, and traumatic brain injuries, wildfire smoke and infection by neurotropic viruses are more ubiquitous and harder to avoid. Therefore, it is crucial to continue research on risk factor mitigation and the pathogenesis of Parkinson's disease. This research requires suitable animal models that closely replicate the disease in humans.

2.1.3 Pathogenesis

PD is primarily characterized by the loss of neuromelanin-containing dopaminergic neurons in the substantia nigra pars compacta (SNpc), a region of the midbrain that plays crucial roles in reward pathways and cognitive functions [49]. As part of the basal ganglia, the SNpc also functions in movement and motor control [49]. The pars compacta is one of the two parts of the substantia nigra and contains neurons that produce dopamine, a neurotransmitter involved in modulation and initiation of voluntary movement, among other effects [49]. As the disease progresses, dopaminergic neurons degenerate and die, causing a decrease in dopamine that leads to movement symptoms such as tremors and rigidity [49]. By motor symptom onset, 30% of the dopaminergic neurons in the SNpc have died based on postmortem brain studies [50][51].

Many molecular processes have been implicated in the pathogenesis of PD, including alpha-synuclein misfolding and aggregation, mitochondrial dysfunction, and dysfunctional protein clearance systems [52]. Alpha-synuclein is a neuronal protein primarily located at the presynaptic terminals of brain neurons [53]. Although its functions are still being fully assessed, research suggests this protein is involved in a wide variety of functions, including synaptic homeostasis and

neurotransmitter release and reuptake [53]. In addition, alpha-synuclein has important immune functions, activating anti-viral interferon responses to viral infection in the brain through activation of JAK/STAT signaling [54]. Abnormal alpha-synuclein protein aggregation has been commonly implicated in PD and other synucleinopathies [53]. Several factors can trigger this aggregation, including oxidative stress and alterations in mitochondrial function, which cause monomers to conformationally change into beta-sheet-rich monomers, oligomeric structures, and larger amyloid fibrils [53]. These fibrils form Lewy bodies, one of the pathological hallmarks of PD and other neurodegenerative diseases such as Alzheimer's disease [53].

More recently, neuroinflammation has been identified as contributing to pathogenesis, rather than a secondary response to the disease itself [52]. Studies utilizing MPTP (1-methyl-4-phenyl-1,2,3,6-tetrahydropyridine) and 6-OHDA (6-hydroxydopamine) rodent models of PD have suggested that inflammatory processes through microglial activation may contribute to the degeneration of dopaminergic neurons in the SNpc, while inhibition of microglial activation may be neuroprotective [55][56]. A study involving human patients also observed that a higher pro-inflammatory immune marker profile is associated with more rapid motor symptom progression and faster cognitive decline and may even represent a potential prognostic indicator [57]. Finally, many studies have linked various environmental risk factors, such as heavy metals, pesticides, and wildfire smoke, to the development of neuroinflammation and their link to PD development [42][58][59].

This neuroinflammation has been shown to lead to neurodegeneration, and ultimately neuronal death [60]. In response to either a damaged neuron or toxins in the CNS, microglia and astrocytes, the resident immune cells of the brain, become activated [60]. These cells release pro-inflammatory cytokines, such as interleukin-1 beta (IL-1β), interferon--γ (IFN-γ), and tumor

necrosis factor alpha (TNF-α) [60]. While these activate various signaling pathways to have neuroprotective effects, chronic stimulation leads to neurotoxic effects [60]. These can directly trigger neuronal injury and death through various mechanisms. Cytokines can affect glutamate signaling by increasing glutamate release and impairing glutamate clearance, leading to excitotoxicity that directly damages neurons [61]. These pro-inflammatory cytokines can also directly promote neuronal apoptosis and contribute directly to oxidative stress by inducing the production of reactive oxygen species in various cell types [62]. Furthermore, cytokines can compromise the integrity of the BBB, indirectly allowing further damage if harmful substances subsequently enter the brain [63].

While inflammation is the body's mechanism for healing damage and protecting the body from pathogens, chronic inflammation becomes deleterious to the body, leading to pathological states such as PD. Understanding the pathological processes involved in the development of PD can inform research on potential therapeutic targets and disease-modifying treatments.

2.1.4 Treatment options

Currently, approved pharmacological treatment options for PD patients are primarily limited to medications focused on symptomatic relief of motor symptoms associated with a decline in dopamine [64]. However, dopamine itself cannot cross the blood-brain barrier (BBB) [64]. Therefore, these medications must target different components of the dopamine biosynthetic pathway, ultimately increasing the amount of dopamine available in the body [64]. The dopamine precursor, levodopa (L-Dopa), is the most widely recognized and successful medication in the treatment of PD [64]. Interestingly, Ayurvedic medicine has a lengthy history of using Mucuna pruriens, a bean that contains L-Dopa in its raw form, dating back to approximately 1500-1000

BC [65]. While medications like levodopa have come a long way in terms of improving safety and efficacy, they have some serious limitations in their applicability to patients.

Firstly, these drugs have serious side effects that must be considered. Levodopa, for example, has side effects secondary to dopamine metabolism outside of the central nervous system by the action of DOPA decarboxylase [64]. The emergence of motor complications such as severe unpredictable fluctuations between stable states and dyskinesias, or involuntary hyperkinetic movements, sparks debate on the benefit of beginning treatment [66]. These side effects can be ameliorated through reducing levodopa dosage or delaying initiation of levodopa treatment [64]. Unfortunately, this forces patients to decide between improving motor function and avoiding adverse effects. More recently, DOPA decarboxylase inhibitors such as carbidopa are compounded with levodopa to reduce peripheral conversion of the drug and therefore detrimental side effects [67]. Researchers are currently continuing to develop other medications and modes of delivery in the hopes of improving clinical efficacy and side-effect profiles [68].

Secondly, because these treatment options only target healthy neurons that can synthesize dopamine, they become less effective over time. Carbidopa users often need to take increasing dosages of the drug even beyond the 800mg dosage limit set by the Food and Drug Administration in 1988 [69]. Because neurons continue to degenerate and die during the progression of PD, dose escalation is required, and side effects become limiting to efficacy, which ultimately reduces quality of life. There are no disease-modifying treatments available currently that reduce the rate of neurodegeneration. Therefore, the major goal of future treatment research is to modify disease progression to slow clinical disability or restore healthy motor function [70][71].

2.2 Viruses as a Risk Factor for Parkinson's Disease

An association between Parkinsonism and numerous viral infections has been demonstrated throughout recent history. The first well-documented occurrence was during the 1918 Spanish H1N1 influenza A pandemic, when neurologist von Economo described an epidemic of parkinsonism from 1917 to 1928 that he described as 'encephalitis lethargica' [72][73]. Postmortem examination of the brains of patients who did not survive the initial phase showed periventricular and midbrain inflammation, particularly in the substantia nigra pars compacta [74]. A significant proportion of those who survived the acute encephalitic stage developed a movement disorder similar to Parkinson's disease, involving dystonia, tremors, and blepharospasm [75]. Although an etiologic connection has not been proven between influenza and Parkinsonian symptoms, an encephalitic viral infection and subsequent neuroinflammation can certainly be a risk factor for Parkinson's disease.

The Spanish influenza pandemic likely represents a delayed, or post-infectious form of parkinsonism, in which symptoms appear months after the infection [76]. These post-infectious parkinsonian syndromes are thought to occur through activating the immune system, either non-specifically or through a targeted immune response to a specific host antigen, resulting in a pathogen-induced autoimmunity or neuroinflammation [76]. Although the immune system serves a critical role in protecting hosts against various pathogens, chronic activation can be detrimental. Persistent viral infections would also fall under this category, driving chronic inflammation and immune responses that ultimately cause immune-mediated neurologic injury [76]. Persistent SARS-COV-2 infection, also known as Long Covid, is suggested to increase the risk of delayed PD through chronic inflammation [77]. Similarly, a study of H1N1 infection in mice resulted in

chronic viral-induced inflammation, specifically persistent microglial activation, which can lead to neurodegeneration [78].

Some viruses can instead induce a para-infectious or immediate form of PD, resulting in motor symptoms days or weeks after the infection [76]. In these cases of viral-induced Parkinsonism, there are two possible routes of pathogenesis. Some viruses are more innocuous, indirectly damaging the nigrostriatal pathway and causing PD by inducing inflammatory, vascular, and/or hypoxic injury [7].

Other RNA viruses are neurotropic, accessing the central nervous system directly and damaging the nigrostriatal pathway associated with PD pathology [76]. There are multiple pathways in which these viruses invade the CNS to cause viral replication and neuronal lysis [76]. Viruses can enter peripheral nerves within the spine or cranium, utilizing axons for transport to the CNS [76]. SARS-COV-2, for example, can enter the hippocampus, thalamus, and medulla oblongata through olfactory nerves [79]. Viruses can cross the blood-brain barrier through various mechanisms, such as disrupting tight junctions between endothelial cells, increasing vascular permeability through inflammatory cytokines, or entering endothelial or immune cells [76]. Venezuelan Equine Encephalitis virus (VEEV) has been shown to utilize caveolin-1 (Cav-1)-mediated transcytosis across an intact BBB to enter the CNS [80]. Finally, viruses can also spread via hematogenous routes throughout the body and enter via the blood-cerebrospinal fluid (CSF) barrier through similar mechanisms [81]. Overall, these neuroinvasive viruses are perhaps the most deleterious of all the viral encephalitic pathogenic mechanisms as they enter the brain directly to cause immediate and massive damage.

To further complicate theories of viral pathogenesis and parkinsonism, multiple types of these pathologic processes can co-occur to contribute to neurodegeneration [82]. In addition to

viruses with a general neurotropism for the CNS, some viruses, such as West Nile Virus, exhibit specific neurotropism for deep gray matter nuclei. WNV in particular has a predilection for the substantia nigra, the likely culprit of parkinsonism secondary to this viral infection [83]. Therefore, while there are viruses that are more innocuous in their resulting parkinsonism, some cause targeted damage specifically to brain regions implicated in PD. This not only makes studying the pathogenesis important but also suggests that one of these neurotropic viruses could be used as a model to study the disease.

2.3 Animal Models of Parkinson's Disease

Modern biomedical research relies on experimental modeling of diseases in non-human subjects to gain crucial understanding of disease etiology, pathophysiology, prognosis, diagnosis, and efficacy of treatment modalities. Extensive research has been conducted on the development of animal models of Parkinson's disease, including mechanisms of disease induction, pharmacologically or via genetic manipulation. Ideally, these models would develop PD pathology reliably and quickly, allowing study of the disease without the protracted duration of actual PD development in humans [84].

Rodents are the most common animal model for studying PD, as they are convenient to care for and have robust experimental and behavioral protocols. Many rodent models are used to study the causes, progression, and pathophysiology of the disease. Researchers can induce nigrostriatal dopaminergic degeneration in mice and rats, which correlates with motor deficits that can be observed and measured through various behavioral assays [85]. Due to their short lifespans, research on chronic conditions can be accomplished in a shorter period compared to other animal models. They are generally easy and inexpensive to obtain and experiment on in large numbers, allowing for the collection of substantial amounts of data, which can advance research goals more

quickly than larger animal models. Physiologically, however, rodent models are less similar to humans.

To more closely mimic disease in humans, non-human primates, especially macaques and marmosets, are used in approximately 10% of PD animal studies [86]. Most of these studies are preclinical trials to establish safety and efficacy before clinical trials in human patients [87]. These Because NHPs are resource-intensive, these models are generally reserved for translational research where rodent models are insufficient to achieve study goals. NHPs share a high degree of genetic, physiological, and developmental similarity to those of humans, making them more suitable for translatable research. Although more closely translatable to humans, NHP research raises more ethical questions compared to rodents used in research due to their high intelligence, social complexity, and potential for pain and suffering in ways that are similar to humans [87]. Depending on the location, there may be more legal protections and public scrutiny surrounding NHP research, which can lead to potential disruptions and delays to the research [87]. Therefore, the appropriate animal species for a research study requires careful consideration and foresight. In many cases, therapeutic studies are first tested and validated in rodents prior to progressing to NHP models in preclinical research.

2.3.1 Neurotoxic Models

Many PD animal models are induced by administering neurotoxins to cause degeneration of dopaminergic neurons. 6-hydroxydopamine, 6-OHDA, is a hydroxylated analogue of dopamine and the first neurotoxin to be discovered and used to induce PD in the 1960s [88]. The underlying mechanisms of this toxicity are oxidative stress and the production of free radicals [89]. This compound does not cross the blood-brain barrier, however, requiring intracerebral injections to establish neurodegeneration in animals [90]. Researchers can target specific areas of the brain,

such as the SNpc, striatum, or medial forebrain bundle [90]. A unilateral deficit model can also be created to observe asymmetric motor deficits and rotational behavior and use the contralateral limb as a control, potentially reducing the number of animals required to complete an experiment [88]. However, bilateral injections cause adipsia, aphagia, seizures, and a high mortality rate [91]. Non-human primate (NHP) models using 6-OHDA have also been used in therapeutic development, but require serial intracerebral injections, raising the risk of surgical complications [92].

The next neurotoxic model of PD, MPTP (1-methyl-4-phenyl-1,2,3,6-tetrahydropyridine), is more commonly used in both mice and NHP. Rats are not commonly used with MPTP, however, as they are resistant to moderate doses, and high doses cause increased mortality [93]. The toxin is lipophilic and crosses the BBB quickly, where it is taken up by glial cells and converted into MPP+ (1-methyl-4-phenylpyridinium) [94]. MPP+ blocks mitochondrial complex I, which reduces ATP production and increases oxidative stress to eventually cause neuroinflammation, neurodegeneration, and neuronal death [94]. In mice, MPTP reliably induces dopaminergic neuronal death in the SNpc via intraperitoneal injection and correlates with motor deficits [95]. However, depending on the mouse strain used, mice exhibit functional recovery within a few days after injection, limiting the plausibility of behavioral studies [96]. In NHP, MPTP is the gold standard for both acute and chronic models of PD, and functional recovery occurs months post-injection [97]. NHP MPTP models closely resemble PD in humans, making them suitable for preclinical research for therapeutic studies [97].

The final category of neurotoxic animal models of PD involves environmental toxins, such as pesticides and herbicides, a more recently discovered area of risk factors for PD. Rotenone and paraquat have both been used to induce oxidative stress and neuroinflammation to induce PD in rodent models. Rats, in particular, have gained popularity in rotenone administration due to reliably

inducing dopaminergic neuronal death in the SNpc and striatum, motor symptoms, and non-motor symptoms such as sleep disturbances [98][99]. Paraquat, on the other hand, is more commonly used in mice, where it induces SNpc dopaminergic neuronal loss [100]. However, these models do not induce striatal changes or motor deficits, making them less useful for behavioral studies [100]. High doses of paraquat also cause pulmonary fibrosis in mice [101]. While this disease process is another important research area, it can further complicate PD research goals. Regardless, models of PD using pesticides and herbicides can enhance our understanding of how these toxins and other environmental factors contribute to the risk of developing PD.

Heavy metals, such as lead and manganese, have also been used in the study of PD as they are known risk factors for the disease. At high doses, manganese induces CNS oxidative stress and damage by crossing the BBB and the blood-CSF barrier in mice [102]. Particularly, the toxin produces pathology in the basal ganglia, including the striatum, and less frequently the substantia nigra [103][104]. Manganese mouse models of PD have also been used to evaluate the treatment efficacy of L-Dopa following inhalation exposure to manganese [105]. Lead, when injected intraperitoneally into rats, also causes loss of dopamine in the striatum, along with deficits in motor coordination and locomotion [106]. In this study, L-Dopa was found to be ineffective at improving these deficits [106]. Although these heavy metals have been more variable in producing pathological changes in rodents, examining the changes induced by a known risk factor of PD can prove valuable in understanding the pathogenesis of the disease.

2.3.2 Genetic Models

Since genetics plays a role in PD pathogenesis, genetic models and manipulations have been used to attempt to reproduce the disease. Although loss of function mutations in the *parkin*, *DJ-1*, and *PINK1* genes cause symptoms in humans, rodent models with knockouts of any or all

of these genes exhibit normal dopamine levels and functioning of substantia nigra [107]. This suggests that these genes may be protective rather than essential for the survival of dopaminergic neurons during the aging process [107]. Transgenic rodent models carrying mutations in key SNCA point mutations show altered neuronal function and α-synuclein protein aggregation, the primary component of Lewy bodies in PD patients [108]. However, these models do not display the dopaminergic neuronal degeneration or motor deficits characteristic of PD [108].

Although purely hereditary forms of PD are rare, rodent models with genetic manipulations can be used to replicate familial PD and some of its pathology. These models can also be used in conjunction with other models to create a more complete recapitulation of the disease. For example, a dual-hit rat model was created using a strain overexpressing SNCA and administering lipopolysaccharide (LPS) to induce inflammation, which triggered dopaminergic neuronal loss specific to the SNpc [109]. Understanding how these genetic mutations react with environmental factors may prove to be an important upcoming area of research.

2.3.3 Viral Models

There are two categories of using viruses as models for PD. Viral vector models can be used to deliver genetic material into specific brain regions of animals, addressing the deficits of genetic knockout and transgenic strains of mice. Many different viral vectors have been developed and used in the study of PD, including lentiviral vectors, herpes simplex vectors, adenoviral vectors, and recombinant adeno-associated viral vectors [110]. When used in rodents, they display more characteristic and reliable changes in the brains compared to genetic models. For example, viral vector a-synuclein models show dopaminergic neurodegeneration and synuclein pathology compared to a-synuclein transgenic mice [110]. While promising for the study of PD pathogenesis,

further development of these models is needed to reduce variability and increase behavioral impairments if they are to be used to test novel therapeutics [110].

Neurotropic viral models may address some of the deficits of viral vector and other models of PD. Japanese encephalitis virus (JEV) induces distinct pathological changes to the SNpc of rats, a loss of tyrosine-hydroxylase (TH) positive neurons, and marked bradykinesia [111]. More recently, alphaviral models of encephalitis have been investigated in other neurodegenerative disorders. Venezuelan equine encephalitis virus (VEEV), for example, could be used in the study of Alzheimer's disease by inducing neurodegeneration and behavioral changes in mice [112]. The potential for alphaviral encephalitic models to expand into the study of PD by exhibiting neuroinflammation and neurodegeneration will form the basis of this thesis.

2.4 Western Equine Encephalitis Virus

Western equine encephalitis virus (WEEV) is a mosquito-borne arbovirus of the genus *Alphavirus* in the family *Togaviridae*. Virions of WEEV are small, spherical, enveloped particles containing one segment of single-stranded, positive-sense RNA [113]. Glycoprotein spikes attach to host cells, allowing entry into the cytoplasm via endocytosis, where endosomes are formed. Once released from the endosome, alphaviral genomic RNA is translated, transcribed, and replicated to initiate the infection [113].

The virus is seen in both North and South America. In the western United States and Canada, it is transmitted by its primary mosquito vector, *Culex tarsalis,* as well as other mosquitoes of the genus *Culiseta* [114]. Here, it circulates enzootically among passerine birds and domestic chickens, through which mammals such as humans and horses can become infected tangentially as dead-end hosts from bites of infected mosquitoes [113].

WEEV is the causative agent of Western equine encephalitis (WEE), a lethal infection of the central nervous system (CNS) in humans and horses. However, the pattern of the disease, disease severity, and incidence vary greatly. There have been sporadic outbreaks in both horses and people from the 1930s through the 1980s in the United States. However, WEEV is currently the rarest among the encephalitic alphaviruses, with Venezuelan equine encephalitis virus (VEEV) and Eastern equine encephalitis virus (EEEV) being more prevalent [115]. No human infections of WEEV have been detected since 1999 in the United States, and fewer than 700 total cases have been reported in the United States since the 1960s [116]. More recent outbreaks have been documented in South America, including one in 2023-2024 in Argentina and Uruguay, which resulted in 217 human infections, 12 fatalities, and 2,548 equine cases [117].

Most of the historically reported cases represent severe forms of the disease that were either lethal or resulted in survivors suffering from permanent neurological sequelae [114]. In reality, the majority of infections are likely either asymptomatic or mild with flu-like symptoms and therefore underreported. The incidence and severity of these symptoms are likely influenced by the viral strain, dose, and route of infection, as well as the age of affected patients [118][119]. Children under 1 year old and adults over 50 years of age are more likely to be affected by severe forms of the disease, with the infant mortality rate being the highest at about 4% [114]. Although mortality rates are generally low for the majority of the population, upwards of 30% of cases develop neurological sequelae. Seizures, decreased motor skills, intellectual and learning disabilities, speech difficulty, altered gait, taste distortion, and loss of facial movements have all been reported in both children and adults after WEEV infection [120]. Interestingly, some of these neurological sequelae, such as motor dysfunction, mirror the symptoms seen in PD patients. More specifically,

a postencephalitic parkinsonian sequelae has been described in patients after confirmed WEEV encephalitis [121].

The similarity of post-encephalitic neurological sequelae of CNS WEEV infection to PD symptoms suggests that WEEV could be used as an animal model to study PD. Initially, an aerosol route of inoculation was used in mice to induce key features of PD, including neuroinflammation, loss of dopaminergic neurons in the SNpc, and α-synuclein aggregation [11]. These mice also displayed neurobehavioral abnormalities and a genetic expression profile correlating to a neurodegenerative phenotype [11]. Astrocytes were also determined to be critical in initiating PD-like pathology following CNS infection with WEEV [12]. A limitation of these intranasal studies, however, was the high morbidity and mortality seen in infected mice within 3-4 dpi, although this may depend on the strain of mouse, strain of virus, and challenge dose [11][12][122]. Adjunctive passive immunotherapy using polyclonal antibodies did improve the survival of mice, allowing the investigation into the long-term effects of CNS WEEV infection [11][12]. One reason for this may be that intranasal inoculation enters the CNS through the olfactory bulb and disseminates into the CNS very quickly, creating multifocal areas of necrosis within 72 hours post-infection [123].

On the other hand, another study comparing infection routes with WEEV in mice determined that footpad inoculation also enters the CNS through hematogenous seeding of circumventricular organs where the BBB is naturally absent [13]. The time to pathology in this study increased to 4-7 dpi for mice infected via footpad injection [13]. Therefore, this route of inoculation with WEEV may lead to a more delayed viral neuroinvasion compared to intranasally infected mice while still resulting in similar histopathologic features. In addition, it is plausible that the systemic immune system may play a role in reducing viral titers from the inoculum before neuroinvasion. While WEEV efficiently spreads directly into the CNS and induces PD-like

pathology, an intranasal model may lead to higher viral titers within the CNS, resulting in morbidity and mortality and requiring immunotherapy [123]. This thesis aims to further investigate the footpad inoculation model of WEEV as an alternative method to intranasal inoculation. The overarching goals of this thesis are to evaluate morbidity and mortality in the footpad inoculation model while still confirming neurodegenerative behavioral and histopathological abnormalities consistent with PD.

CHAPTER 3 – ESTABLISHING OPTIMAL DOSING FOR SUBCUTANEOUS INNOCULATION OF WESTERN EQUINE ENCEPHALITIS VIRUS INTO THE FOOTPADS OF MICE

3.1 Aim

The objective of this study was to establish an optimal dose in plaque-forming units (PFU) for injection of Western equine encephalitis virus (WEEV) into the footpads of mice. Previous studies using intranasal inoculation of WEEV at a dose of 1 x 10^4 PFU to induce Parkinson's disease in mice caused a severe encephalitic infection with rapid propagation of virus throughout the CNS, resulting in significant morbidity requiring euthanasia and mortality in a majority of animal subjects by 4 dpi [11]. Passive immunotherapy targeting the E1-glycoprotein of WEEV was then necessary to improve animal survivability and to characterize the long-term neurological consequences of infection with this alphavirus [11]. This study aimed to determine an optimal dose for footpad inoculation with WEEV that reduces this morbidity and mortality while still displaying key behavioral and histopathologic features of PD.

3.2 Methods

3.2.1 Animals

Male and female C57BL/6 mice of various ages, ranging from 12-week-old to 10-month-old, were reassigned from a breeding colony for this study. All animals were housed in a biosafety level 3 (BSL-3) facility at the Infectious Disease Research Center at Colorado State University for the duration of the study in accordance with institutional health and safety guidelines. Mice were housed socially in commercial individually ventilated cages (Techniplast IVC) filled with small corn cob bedding that was autoclaved prior to use. A commercial irradiated laboratory rodent chow

(Teklad Global) and tap water filtered via reverse osmosis in autoclaved water bottles were available *ad libitum.* The animals were housed under standard conditions, i.e., in a temperature-controlled room maintained at 22-24ºC with 50-70% humidity and a 12:12 hour light: dark cycle. Mice were randomly assigned to control and treatment groups. All mice were handled in compliance with the PHS policy and Guide for the Care and Use of Laboratory Animals. All animal protocols used in this study were reviewed and approved by the Animal Care and Use Committee at Colorado State University. Our institution is an AAALAC-accredited facility.

3.2.2 Experimental design

In pilot 1, 3 doses of virus (0.5×10^4, 1×10^4, 2×10^4 PFU) were tested in accordance with the published intranasal inoculation dosing of 1×10^4 PFU. Each viral group consisted of five mice, with two used as saline controls. Weights and behavioral data were collected at the following time points: 0, 4, 7, 14, 21, and 42 dpi (Figure 3-1). Three mice from each group were euthanized at 14 dpi, and two from each group were euthanized at 42 dpi for histopathology to evaluate viral progression. In pilot 2, viral dosing was increased 10-fold (0.5×10^5, 1×10^5, 2×10^5 PFU) to attempt to induce more significant behavioral and histopathological features. Each viral group consisted of six mice with five saline controls. Weights and behavioral data were collected at the following time points: 0, 4, 7, 14, 21, and 28 dpi (Figure 3-1). The final time point was reduced in pilot 2 due to mortality seen associated with anesthesia.

3.2.3 Viral infection

Mice were anesthetized with isoflurane and inoculated with McFly Luciferase-expressing recombinant WEEV (3'ds WEEV McM fluc McFly B0>B1 2nd Pass) via hind footpad injection at the following concentrations for the first pilot: 0.5×10^4, 1×10^4, 2×10^4 and at the following

concentrations for the second pilot: 0.5 x 10^5, 1 x 10^5, and 2 x 10^5 PFU (Figure 3.2). In pilot 1, the virus was diluted with sterile saline to reach a volume of 20 µL, and this volume was inoculated subcutaneously into the plantar surface of the left hind footpad using an insulin syringe (VetOne VetriJec U-100, 0.5-inch x 29G, 0.3-cc). Control animals were given 20 uL of 0.9% sterile saline (Hospira) into the left footpad. In pilot 2, the virus was diluted with sterile saline to reach a volume of 70 µL, and 35 µL of this solution was injected into each hind foot. This was done because the maximum volume recommended for footpad injection in a mouse is 50 µL per foot to prevent leakage of virus [124]. Control mice were given 35 uL of sterile saline into each hind foot. Mice were examined twice a day for the first seven days post-infection, then once a day for the remainder of the study. Mice presenting in concerning states, i.e., reluctance to move, hunched posture, decreased eating or drinking, or in moribund states, were euthanized. All mice were euthanized by decapitation following isoflurane overdose for fresh brain tissue collection.

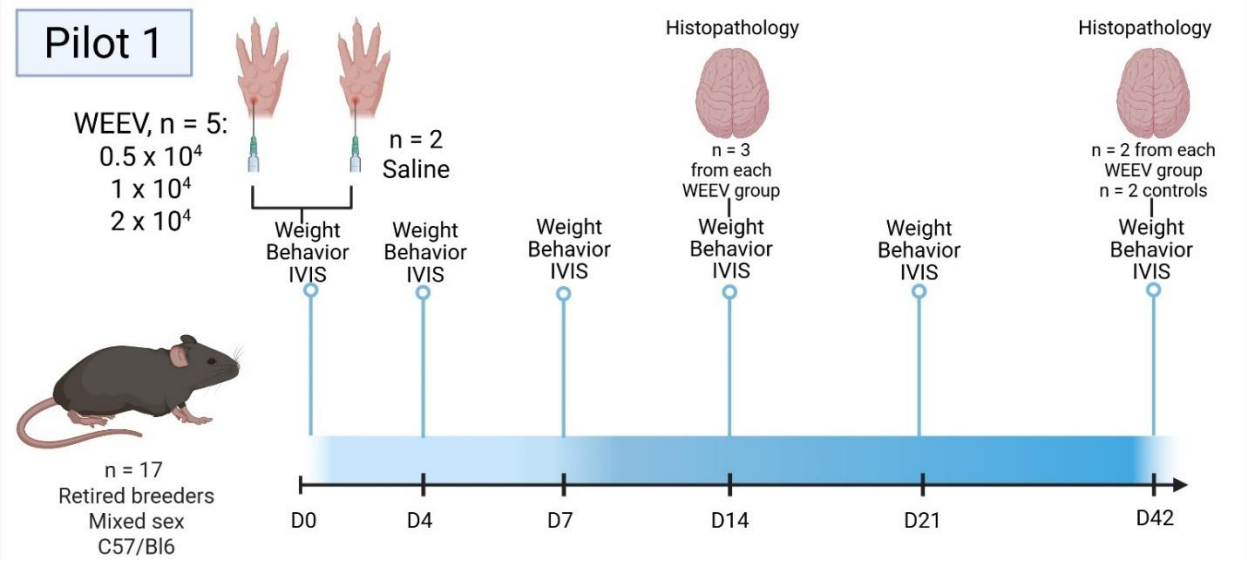

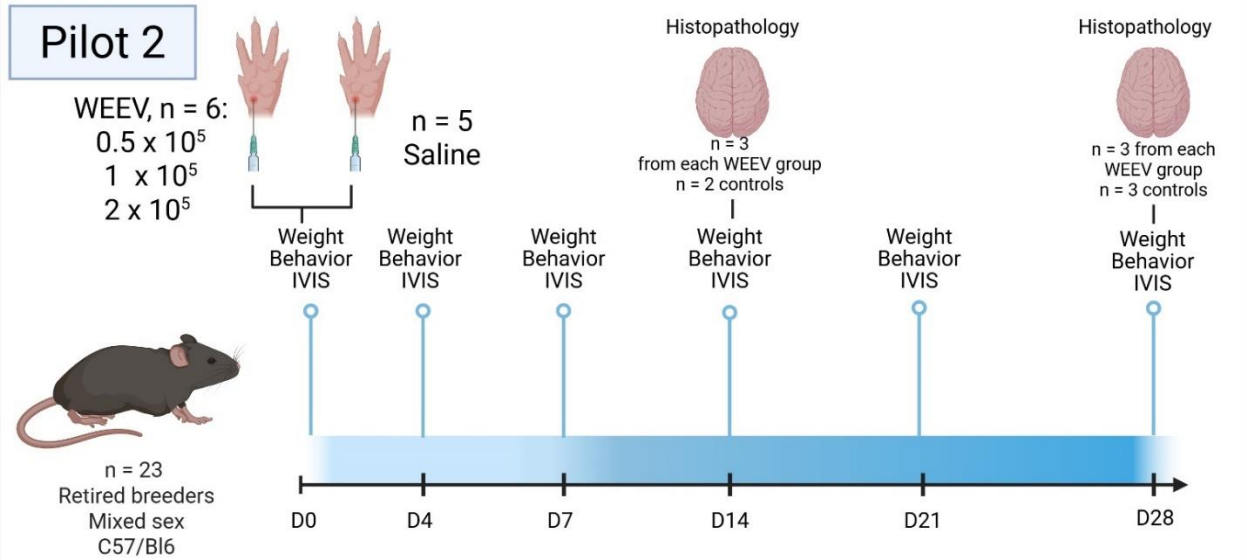

Figure 3-1 Experimental Timelines for Pilot 1 and Pilot 2. Created with BioRender.com.

3.2.4 Weights and behavioral testing

Body weight was collected at each time point using a standard benchtop scale (PCE Instruments) with a tared plastic cylinder to contain the mouse. The pole test has been used in other studies to assess motor function in mouse models of basal ganglia-related movement disorders [125]. Briefly, animals were placed at the top of a laboratory support stand with a self-made vertical metal rod 50 cm long and 1 cm in diameter within the base of the home cage and released. The time to descend the pole from top to bottom was recorded until the mouse fully released the pole with all four paws. In addition to the pole test, a hang test, also known as an inverted grid test, was utilized to measure grip strength and motor coordination [126]. A wire mesh grid (12 x 12 cm) with 25 mm^2 openings was utilized. Each mouse was placed in the center of the grid over their home cage, which was then turned upside down so the mouse was hanging and clinging onto the grid. The distance between the grid and the home cage was approximately 25 cm to cushion their falls and prevent escape. When a mouse reached the edge of the grid, a piece of cardboard was

used to prevent the mouse from climbing over the edge. The time to fall was recorded with a maximum hang time of 3 minutes. The trial was terminated once the mouse fell off the grid or reached the maximum time limit. The trial was repeated after a one-minute rest period if a mouse attempted to hoist itself up the side of the grid before the cardboard was able to block them. Tests were performed in the following order: weight, pole test, and hang test with at least a one-minute rest period in between each test.

3.2.5 Bioluminescence imaging

Mice were anesthetized with isoflurane (Minrad Inc., Bethlehem, PA, USA) at 2.5% through an XGI-8 anesthesia system (Caliper Life Sciences, Waltham, MA, USA) connected to the IVIS 200 (Caliper Life Sciences, Waltham, MA, USA) imaging camera system. Mice received 150 mg/kg luciferin substrate (30mg/mL stock diluted in PBS) subcutaneously 10-15 minutes before imaging. Mice were imaged for 20 minutes total at each time point. Uninfected mice were used as an imaging control to adjust for background signal. A standard region of interest (ROI) was created around each head and left hind footpad to measure total light emission for each mouse. Living Image 3.0 software (Caliper Life Sciences, Waltham, MA, USA) was used to process the images taken using the IVIS 200. In Pilot 2, the dorsal surfaces of the heads of the mice were shaved to determine if the fur affected the fluorescent signaling picked up by the IVIS.

3.2.6 Tissue processing and sectioning

Brains were carefully and quickly removed following decapitation within a Class II A2 biosafety cabinet and fixed in 10% neutral buffered formaldehyde (Fisher Scientific) in conical tubes. Tissues were incubated for a minimum of 14 days at room temperature within the BSC to ensure deactivation of the virus within tissues in accordance with approved biosafety protocols.

Brains were embedded in paraffin wax by a diagnostic laboratory (ClearCut Research, Boulder, CO). SNpc samples were sectioned at 24 μm thickness in pilot 1 and 8 μm thickness in pilot 2 on a microtome through the anatomic midbrain and mounted on glass slides.

3.2.7 Staining and imaging of striatal neurons

Coronal striatal sections were deparaffinized and stained using anti-tyrosine hydroxylase (TH; 1:500; Millipore AB152) to identify TH-positive dopaminergic neurons and 4',6-diamidino-2-phenylindole (DAPI, Sigma) to identify nuclei per previously established methods. Sections were mounted on glass slides and visualized using an automated Olympus Bx63 fluorescence microscope, Hammatsu Flash4.0 digital CMOS camera, ProScan III stage controller (Prior, Rockland, MA, USA), and CellSens Dimension software (version 1.12, Olympus, Center Valley, PA, USA). All slides for each pilot were stained and imaged simultaneously to reduce variability in intensity measurements. ROIs specific to the striatal brain regions were applied using a reference to a coronal atlas of the mouse brain (Allen Brain Atlas). Total average fluorescence intensity was determined using manual threshold masking within the CellSens platform.

3.2.8 Staining, imaging, and stereological assessment of substantia nigra neurons

Coronal substantia nigra sections were deparaffinized and stained using anti-tyrosine hydroxylase (TH; 1:500; Millipore AB152) to identify TH-positive dopaminergic neurons, 4',6-diamidino-2-phenylindole (DAPI, Sigma) to identify nuclei and hexaribonucleotide binding protein-3 (NeuN) as a secondary neuronal marker, per previously established methods. Sections were mounted on glass slides and visualized using an automated Olympus Bx63 fluorescence microscope, Hammatsu Flash4.0 digital CMOS camera, ProScan III stage controller (Prior, Rockland, MA, USA), and CellSens Dimension software (version 1.12, Olympus, Center Valley,

PA, USA). Methodologies for imaging and counting dopaminergic neurons and total neurons in the substantia nigra were adapted from previous studies [11]. One hemisphere of each section was quantified by creating anatomically specific ROIs based on TH immunolabeling and a reference to a coronal atlas of the mouse brain (Allen Brain Atlas). All images were obtained and analyzed under the same conditions for magnification, exposure time, LED intensity, camera gain, and filter settings to minimize variability in intensity measurements. Stereological analysis of dopaminergic neurons in the SNpc was then performed as described in previous studies and according to recent methods [11]. TH-positive and NeuN-positive soma from selected ROIs were counted using adaptive thresholding in the Count and Measure feature on the Olympus CellSens platform. Each soma was also verified to be DAPI-positive to confirm that only nuclei were included in counts.

3.2.8 Statistical analysis

Statistical analysis was performed using Prism (v5.0; GraphPad Software, San Diego, CA). Data was presented as the means +/- standard error of the mean (SEM) unless otherwise noted; $P < 0.05$ was considered significant. Experimental values from each mean were analyzed with a ROUT (alpha = 0.05) test to identify and exclude significant outliers. Differences between each experimental group were analyzed using an unpaired t-test or repeated measures two-way ANOVA and Šidák's correction for multiple comparisons, and described in figure legends.

3.3 Results

3.3.1 Systemic WEEV may cause dose- and time-dependent deficits in motor coordination and difficulty recovering from prolonged anesthesia

Weights were obtained on mice at each time point to monitor their overall health status in addition to frequent observations for morbidity and mortality. At all viral doses, the weights of the

mice remained relatively static (Figure 3-2 A and 3-3 A). Mice did not exhibit any clinical signs, such as depression, lethargy, or weight loss, in either study. No mortality occurred in mice in pilot 1. In pilot 2, 2 mice in the 0.5 x 10^5 PFU group, 2 mice in the 1 x 10^5 PFU group, and one mouse in the 2 x 10^5 PFU group did not recover from anesthesia, which required euthanasia (Figure 3-3 B).

Behavioral testing was performed to evaluate motor deficits in infected mice. Firstly, the pole test was used to measure motor coordination during the descent of a metal pole. In pilot 1, the pole test showed a prolonged latency to descend the pole in the 0.5 x 10^4 PFU group at 21 dpi compared to the control group, although this was not statistically significant (Figure 3-2 B, p=0.2912). All other groups showed some variability in their pole test results but remained similar to the control group. The fixed effects model revealed a significant effect of dpi on latency to descend (p=0.289) and a significant effect of dpi and PFU on latency to descend (p=0.0024). In pilot 2, mice in the 0.5 x 10^5 PFU group descended the pole significantly faster at 14 dpi compared to baseline and 3 dpi (Figure 3-3 C, p=0.0494 and p=0.0416, respectively). Similarly, all other groups showed some variability, namely a decrease in latency to descend at 14 dpi in the 1 x 10^5 group compared to controls, but these changes were not statistically significant (p=0.1354). The fixed effects model revealed a statistically significant effect of dpi on latency to descend (p=0.0123). These changes may be indicative of time- and dose-dependent deficits in motor coordination.

The results of the hang test showed the most variability. In pilot 1, control mice struggled to hang on to the grid at baseline, indicating that they needed additional time to acclimate to the test (Figure 3-2 C). While infected groups showed some variability in their latencies to fall, their results were similar to those of control mice (p>0.95). In pilot 2, an observable decrease in latency

to fall was seen in the 1 x 10^5 PFU group at 28 dpi compared to controls, although this change was not statistically significant (Figure 3-3 D, p=0.3208). All other infectious groups remained similar to the control group across all time points.

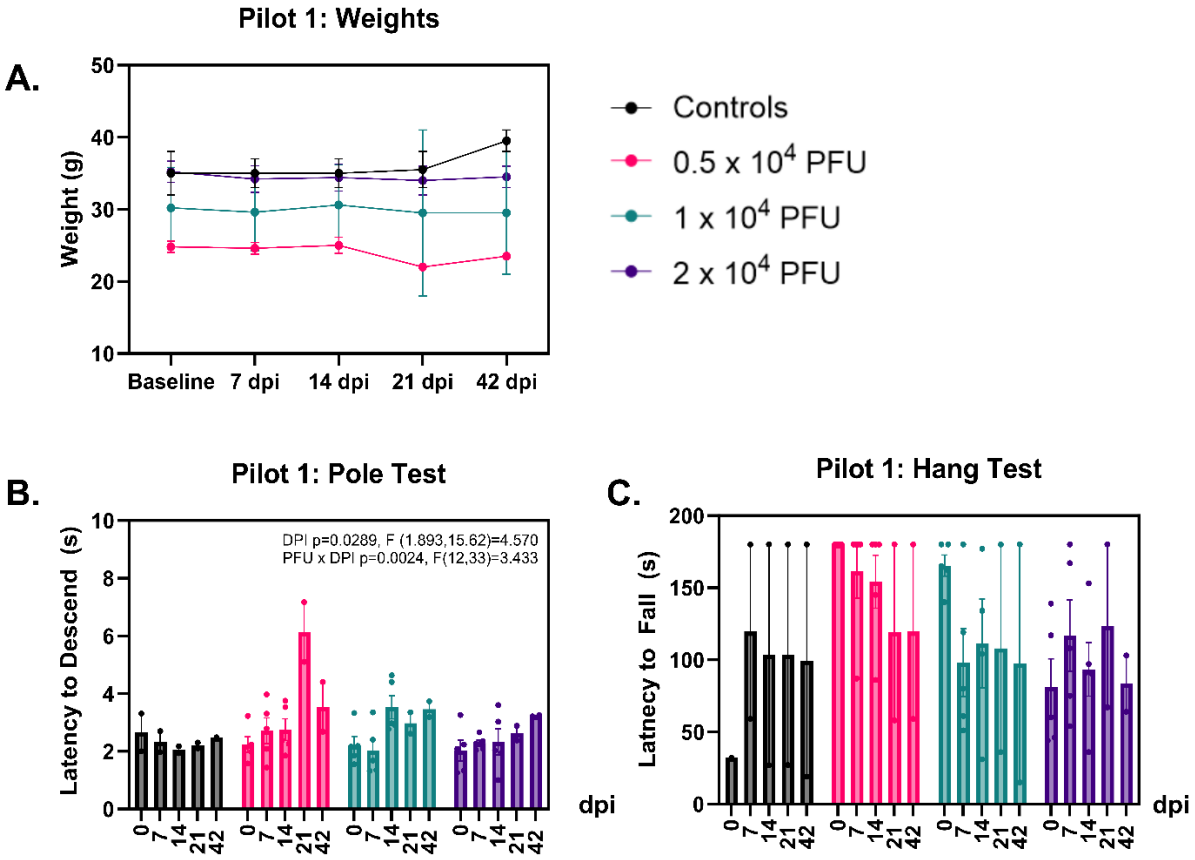

Figure 3-2 Weight, Pole Test, and Hang Test data for Pilot 1. Effect of systemic WEEV on weight (A), pole test (B), and hang test (C). Statistical analysis was performed using Two-Way ANOVA, multiple pairwise comparisons, displayed in mean +/- SEM.

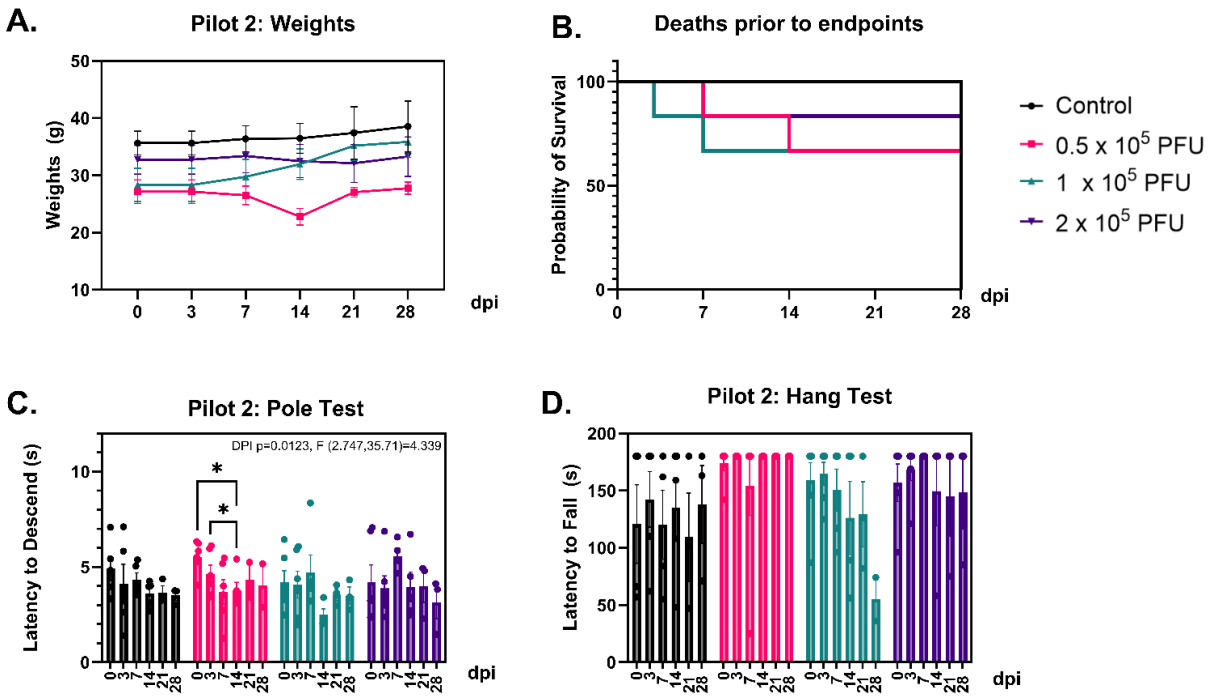

Figure 3-3 Weight, Survival, Pole Test, and Hang Test Data for Pilot 2. Effect of systemic WEEV on weight (A), survival (B), pole test (C), and hang test (D). Statistical analysis was performed using Two-Way ANOVA, multiple pairwise comparisons, displayed in mean +/- SEM (*p<0.05).

3.3.2 WEEV exposure results in positive bioluminescent imaging in inoculated footpads and brains

Bioluminescent imaging was used to verify viral activity in the footpads and brains of infected mice. In pilot 1, mice showed positive bioluminescence only in their footpads (Figure 3-4 A). In pilot 2, the heads of the mice were shaved to determine if the dark fur of the C57BL/6 mice was obstructing the bioluminescent signaling picked up by the IVIS camera. Here, we saw reactivity in the heads of some of the mice (Figure 3-4 B). As expected, no luminescence was detected in the heads or footpads of any of the uninfected control mice (Figure 3-4 C). While these results were sufficient to determine positive systemic viral infection, they were inconsistent in determining positive CNS infection. These results were also obscured by the malfunctioning of the IVIS camera during pilot 2 data collections at the 14 dpi time point and beyond. Therefore,

bioluminescence values were not analyzed for either of these pilot studies due to the unreliability of these results.

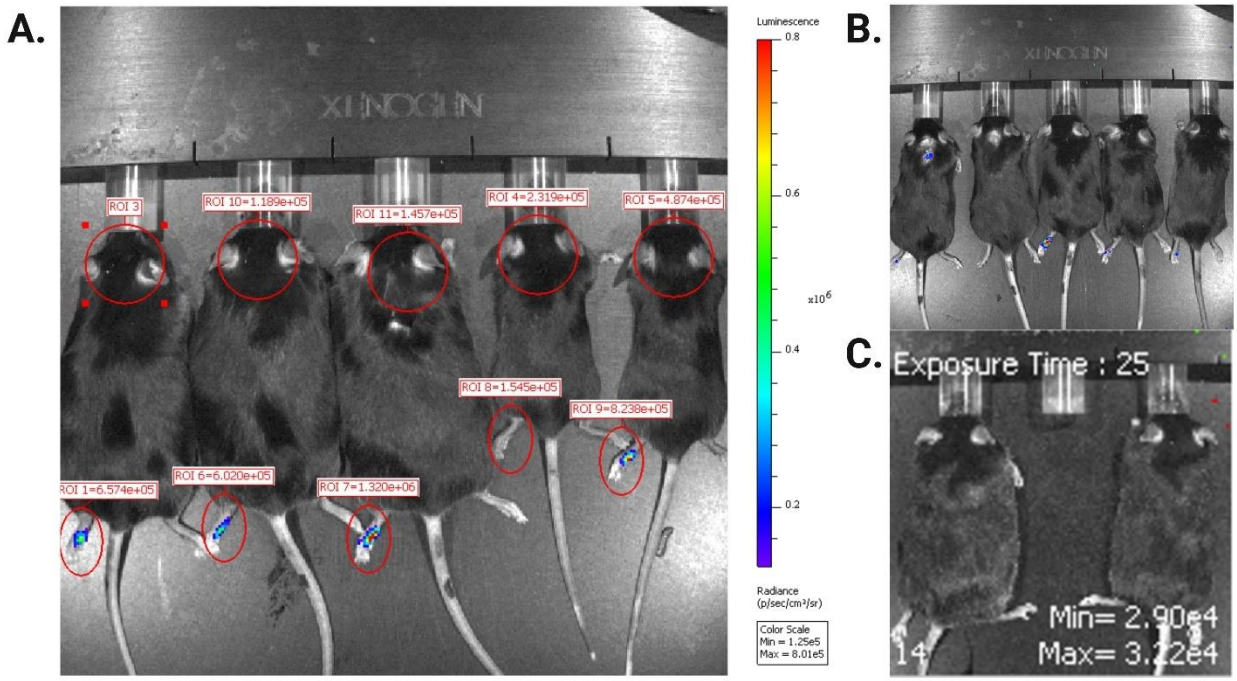

Figure 3-4 IVIS Imaging. A. Pilot 1, Displaying mice inoculated with 1 x 10^4 PFU imaged at 14 dpi. Positive reactivity of luciferase was observed in the hind footpads of mice that were inoculated. Luminescence measurements range from 1.545 x 10^5 and 1.32 x 10^6 in the footpads and 1.189 x 10^5 and 4.874 x 10^5 in the heads. B. Pilot 2, Displaying mice inoculated with 2 x 10^5 PFU imaged at 28dpi. Positive reactivity was observed in the hind footpads of mice and the head of one mouse. C. Pilot 1, Control mice imaged at 28dpi. No luminescence detected in heads or footpads. Luminescence scale ranged from 2.90 x 10^4 and 3.22 x 10^4.

3.3.3 Systemic WEEV causes progressive loss of dopamine in the striatum

Histopathological changes in striatal sections of the brain were analyzed to determine if WEEV infection induces a decrease in striatal dopamine. On histopathology slides stained with TH and DAPI, patches of decreased staining intensity can be visualized in infected mice compared to control mice in both pilot 1 and pilot 2 (Figure 3-5B, C, E, F). Quantification of striatal dopamine was determined through measuring the expression of TH intensity, an indicator of dopaminergic

activity, in this brain region. In pilot 1, a significant decrease in mean striatal TH intensity is seen across all viral dosing groups (Figure 3-5 A, $p<0.0001$). In pilot 2, a significant decrease is also seen in all viral dosing groups at 14 dpi compared to controls (Figure 3-5 E, $p=0.0393$ for 50,000 PFU, $p<0.0001$ for 100,000 and 200,000 PFU), and at 42 dpi (Figure 3-5E, $p=0.0012$ for 50,000 PFU, $p=0.0009$ for 100,000 PFU, and $p=0.0002$ for 200,000 PFU).

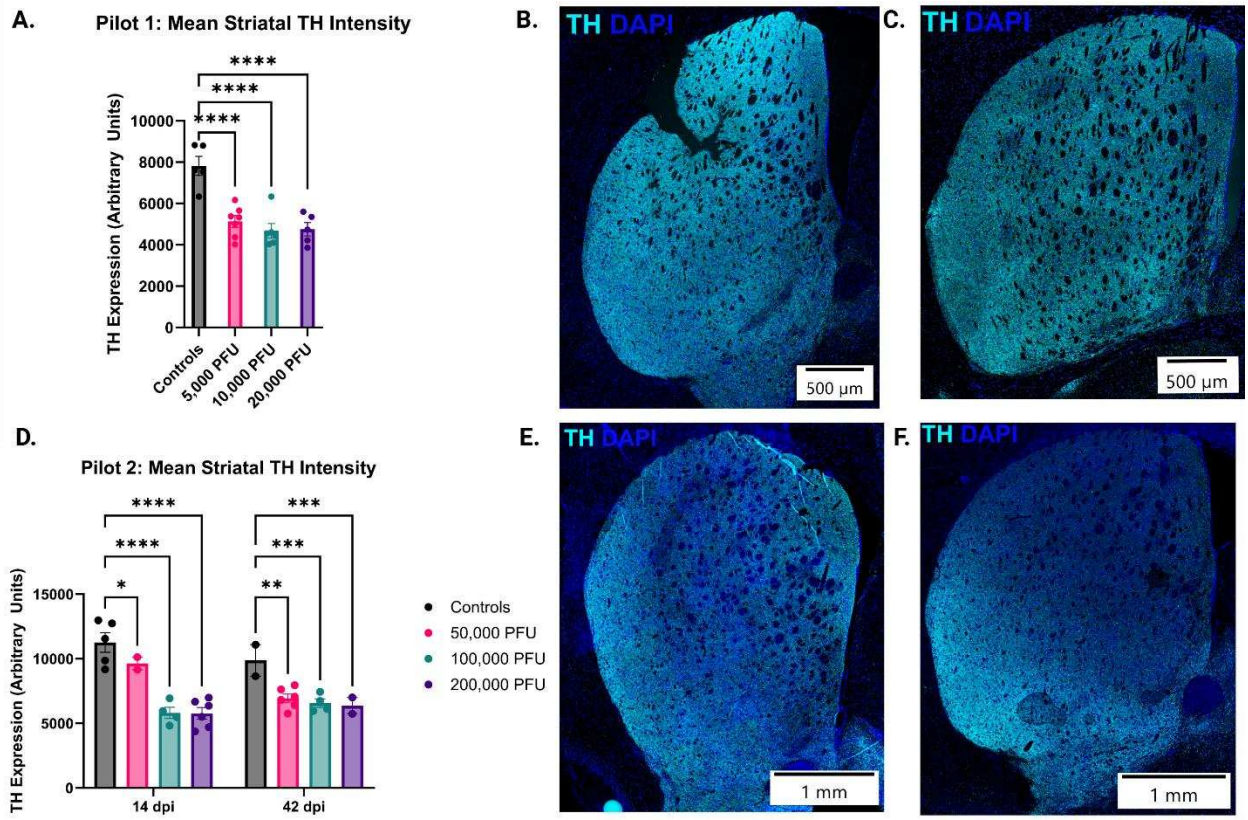

Figure 3-5 Quantification of neuronal loss in the striatum. Decreased striatal TH intensity is seen in pilot 1 infected mice (A) and pilot 2 infected mice (D) compared to their respective control groups. Representative images of striatum for pilot 1 controls (B) and 0.5 x 10^4 PFU infected mice (C), and representative images for pilot 2 controls (E) and 0.5 x 10^5 PFU infected mice (F). Statistical analysis was performed using Two-Way ANOVA, multiple pairwise comparisons, displayed in mean +/- SEM (*$p<0.05$, **$p<0.01$, ***$p<0.001$, ****$p<0.0001$)

3.3.4 Systemic WEEV causes progressive neuronal loss in substantia nigra pars compacta

Histopathological analysis was performed on sections of SNpc to evaluate the loss of dopaminergic neurons. There is a visible decrease in the number of dopaminergic neurons stained for TH, shown in red, and the length and extent of their projections in infected mice compared to control mice in both pilot studies.

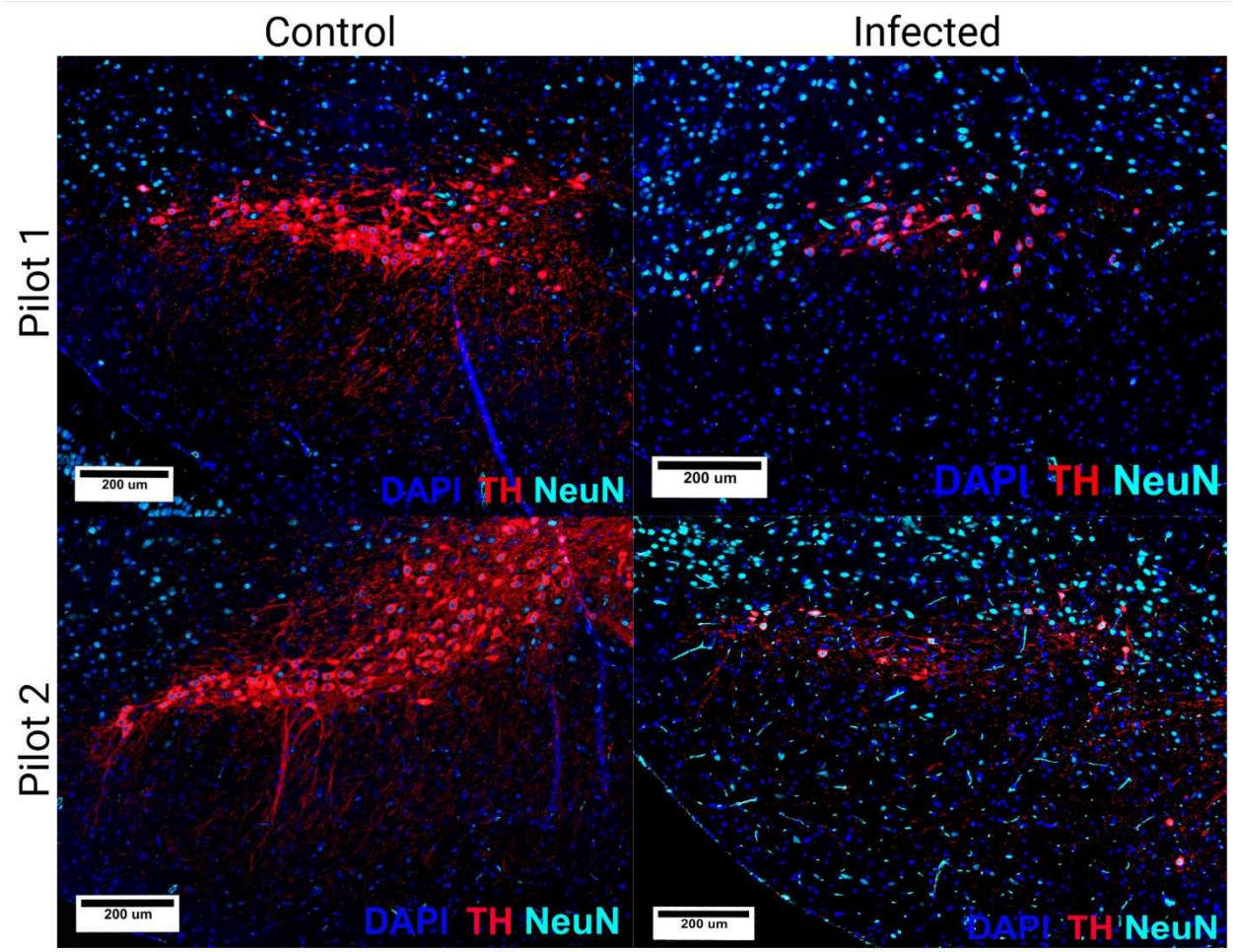

Figure 3-6 Neuronal loss in the substantia nigra pars compacta. Representative images of the substantia nigra pars compacta of pilot 1 control mice vs. 0.5 x 10^4 PFU infected mice, and pilot 2 control mice vs. 0.5 x 10^5 PFU infected mice.

3.4 Discussion

Mice did not exhibit any morbidity or mortality in the first pilot study. Similarly, no animals displayed any clinical signs of infection in pilot 2. However, some mice did not recover from anesthesia and required euthanasia. Because these euthanasias were correlated with anesthesia, we hypothesize that infected mice were more sensitive to the lengthy anesthesia of the IVIS imaging, causing them to have more trouble waking up. Isoflurane and other volatile general anesthetics can modulate the immune system, which could acutely alter disease progression [127]. Although isoflurane is generally considered to be a safe anesthetic, one study found that isoflurane usage in rodent models has antioxidant and anti-inflammatory effects on various cells except for neuronal cells [128]. Isoflurane may contribute to neuronal injury and death in other rodent models of disease [129]. Therefore, it is plausible that isoflurane itself, especially when administered for 20 minutes, may aggravate the neurologic phenotype in our mouse model. Because the IVIS camera started to malfunction at 14 dpi, the machine was not utilized for the rest of the study, and further euthanasias were not required. This further suggests a correlation between these euthanasias and sensitivity to anesthesia.

The pole test is designed to track impairments to motor coordination and sensorimotor impairments associated with hypothalamic and nigrostriatal motivation systems in rodents [125]. While the pole test showed some changes in the lowest viral dose groups in both pilot 1 and pilot 2, these results were inconsistent across all viral groups. Some researchers using the pole test create a rougher surface to improve the ability of the mice to grip the pole, either by adding an adhesive material to a metal pole or using a wooden pole [130][131]. We hypothesize that the variability seen in our pole test results is secondary to the difficulty of the mice gripping the bare metal pole.

A refinement to this technique in our next aim will be to wrap the metal pole with an adhesive material to improve its ability to be gripped, which may therefore produce more accurate results.

We also noted a high degree of variability in our hang test results. The hang test, although simple and easy to do in a biological safety cabinet, can be highly stressful for the animal [126]. In addition, some mice in our study reached the edge of the grid and attempted to hoist themselves up the side before the piece of cardboard was able to block them, requiring repetition of the trial and adding to the animal's fatigue. A refinement for this technique would be to utilize a grid with sides to prevent climbing over the edges. It is also important to consider the effect of the slight movements of the person holding the grid. Even small movements and vibrations from the observer's hands and arms can affect the ability of the mouse to hang on. Some studies utilize a grid that is mounted on metal rods so that it can be rotated 180 degrees, eliminating the need for a human holder [126]. Finally, the hang test ultimately measures a mouse's ability to sustain their grip over time. This can help to estimate muscular strength and coordination, but it is ultimately a test of endurance. Due to these facts, we conclude that the variability seen in the results of our hang test is due to the limitations of the test itself. Therefore, in our second aim, we chose to forgo this behavioral test in favor of a grip strength meter, a more accurate, specific, and validated test for grip strength. Other behavioral tests, including the elevated plus maze, a challenge beam, and a motorized trackway to monitor foot placement, are also excellent tests for determining behavioral phenotypes in mice [132]. However, these tests were not accessible in this study due to biocontainment requirements.

Striatal TH intensity decreased significantly across all viral groups in both pilot studies when compared to control groups. This indicates that systemic WEEV induces loss of dopamine in the striatum, a key histopathologic feature of PD due to diminishment of dopaminergic

projections from the SNpc. Visually, there is a distinct loss of dopaminergic neurons in the SNpc as well as the length and extent of their projections, representing neuronal loss and loss of projections to the striatum. Both of these key histopathological features represent parkinsonian pathology occurring in infected mice.

While the histopathologic characteristics of PD were achieved in this study, a clear behavioral phenotype could not be determined. This may be due to the limitations of the hang test. In addition, the pole may need to be wrapped with an adhesive to improve mouse traction when descending the pole. Finally, it is not clear if the mortality seen in the study mice was directly related to anesthesia. In the subsequent study, a grip strength meter replaced the hang test to more accurately determine grip strength, and the pole was wrapped to prevent mice from slipping down the pole. In addition, because the IVIS malfunctioned, anesthesia was not utilized, which will help to uncover the correlation between mortality and anesthesia in this study.

CHAPTER 4 – EXAMINING BEHAVIORAL CHARACTERISTICS OF MICE INFECTED WITH WESTERN EQUINE ENCEPHALITIS VIRUS

4.1 Aim

This study aimed to fully characterize this mouse model of footpad infection with Western equine encephalitis virus (WEEV) at a dose of 2 x 10^5 PFU through behavioral analysis.

4.2 Methods

4.2.1 Animals

Thirty-two 8-week-old C57BL/6 mice were purchased from Charles River Laboratories. All animals were housed in a biosafety level 3 (BSL-3) facility at the Infectious Disease Research Center at Colorado State University for the duration of the study in accordance with institutional health and safety guidelines. Mice were housed socially in commercial individually ventilated cages (Techniplast IVC) filled with small corn cob bedding that was autoclaved prior to use. A commercial irradiated laboratory rodent chow (Teklad Global) and tap water filtered via reverse osmosis in autoclaved water bottles were available *ad libitum*. The animals were housed under standard conditions, i.e., in a temperature-controlled room maintained at 22-24ºC with 50-70% humidity and a 12:12 hour light: dark cycle. Mice were randomly assigned to control and treatment groups. All mice were handled in compliance with the PHS policy and Guide for the Care and Use of Laboratory Animals. All animal protocols used in this study were reviewed and approved by the Animal Care and Use Committee at Colorado State University. Our institution is an AAALAC International-accredited facility.

4.2.2 Experimental design

In this study, a single viral dose (2×10^5 PFU) was administered to 16 mice. An equal number of control mice were administered saline. Weights and behavioral data were collected at the following time points: 0, 4, 7, 14, 21, and 42 dpi (Figure 4-1). Half of the mice were euthanized at 14 dpi, and the other half were euthanized at 42 dpi for plaque assays to confirm viral infection and histopathology samples for future analysis

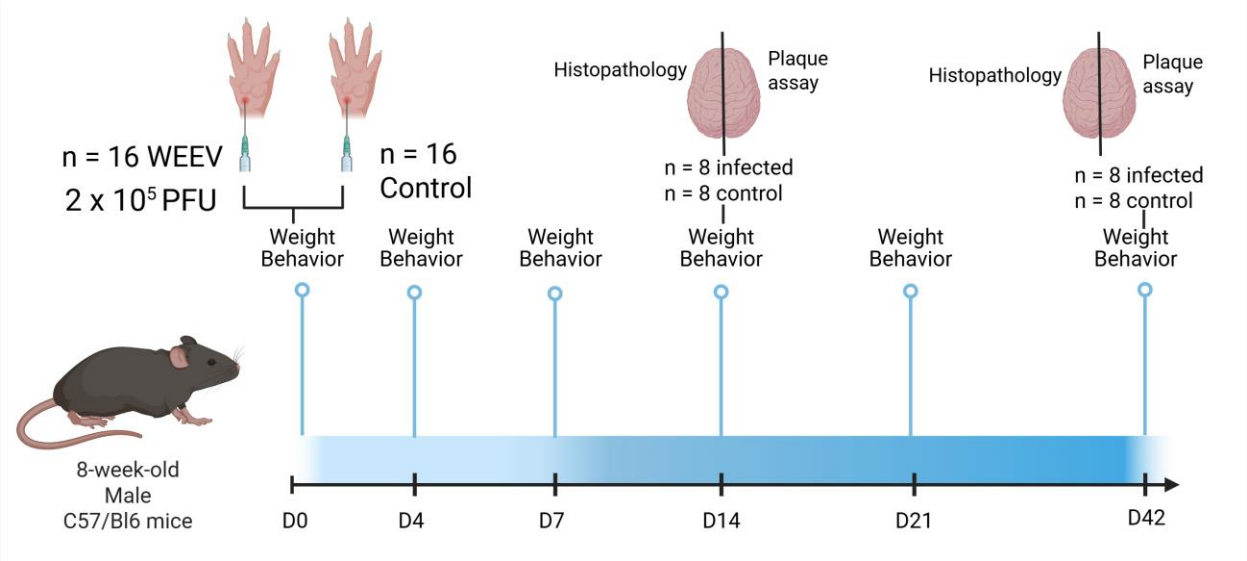

Figure 4-1 Experimental Timeline. Created with BioRender.com

4.2.3 Viral infection

Mice were anesthetized with isoflurane (Minrad Inc., Bethlehem, PA, USA) and inoculated with McFly Luciferase-expressing recombinant WEEV via left hind footpad injection at a concentration of 2 x 10^5 PFU. When the injection volume exceeded 50 µL, the remainder was administered into the right hind footpad. Mice were examined twice a day for the first seven days post-infection, then once a day for the remainder of the study. Mice presenting in concerning states, i.e., reluctance to move, hunched posture, decreased eating or drinking, or in moribund states, were

euthanized. All mice were euthanized by decapitation following isoflurane overdose for fresh brain tissue collection.

4.2.4 Weights and behavioral analysis

A weight was collected at each time point using a standard benchtop scale with a tared plastic cylinder to contain the mouse. The pole test was conducted in accordance with the previous chapter. Unlike the pilot studies, the rod was wrapped in a veterinary self-adhering fabric bandage (Andover Healthcare) to provide extra grip to the animals and more accurately measure the degree of bradykinesia.

Grip strength meters have also been used in similar neurodegenerative studies [133]. The force of grip strength was measured using a computerized grip strength meter (Maze Engineers, USA). The apparatus consists of a baseplate, a trapezoidal stainless-steel grip, and a force sensor. Each subject was gently lifted at the base of the tail such that both its forepaws or all four paws could grasp onto the steel grip. The subject was then pulled away from the apparatus by the tail parallel to the countertop until it released its grip. The peak tensile force of each trial was automatically measured in grams of force (gF). A one-minute resting period was allowed between trials, and three trials of foregrip and three trials of all four paws were performed for each subject. Testing was performed in the following order: weight, pole test, forelimb grip strength, and forelimb and hindlimb grip strength. All behavioral testing was performed on uninfected and infected mice on days 0 and 3, then weekly until the animal's endpoint.

4.2.5 Tissue processing and sectioning

Brains were carefully and quickly removed following decapitation within a Class II A2 biosafety cabinet and fixed in 10% neutral buffered formaldehyde (Fisher Scientific) in conical

tubes. Tissues were incubated for a minimum of 14 days at room temperature within the BSC to ensure deactivation of the virus within tissues in accordance with approved biosafety protocols. One hemisphere of each brain was embedded in paraffin wax by a diagnostic laboratory and cut into 10 μm transverse coronal sections on a microtome through the anatomic midbrain and mounted on glass slides for future analysis.

4.2.6 Plaque assays

The other hemisphere of each brain was grossly dissected for striatum to be used for neurochemistry analysis. Remaining tissues were quantified for infectious virus using plaque assay. Fresh-frozen brain tissues were homogenized for 30 seconds at a frequency of 30 revolutions per second using a stainless-steel bead (Qiagen TissueLyser II). Monolayers of Vero cells (ATCC® CCL-81™) were seeded on 12-well tissue culture plates to 90-100% confluency at a density of 5 x 10^4 cells per well using Dulbecco's Modified Eagle Medium (DMEM, Gibco) supplemented with 5% Fetal Bovine Serum (FBS) and 1% Pen/Strep (Fisher Scientific). Cells were infected with 1:10 serial dilutions of the infected groups and without dilution for control groups. Plates were incubated at 37 ^oC for 1 hour with gentle rocking every 10 minutes. An overlay of 2% agarose and 2% FBS was added, and the plates were incubated at 37 ^oC and 5% CO_2 for 48 hours. For fixing, each well was overlaid with 10% formalin and incubated at room temperature for 30 minutes. The fixed monolayer was then stained with a solution of 20% ethanol in water and 0.25% crystal violet. Plaques were quantified, and viral concentrations were recorded as PFU/mL.

4.2.7 Neurochemistry quantification

Striatal samples were shipped overnight on dry ice to the Neurochemistry Core Laboratory at Vanderbilt University for quantification of monoamine neurotransmitters and their metabolites using high-performance liquid chromatography (HPLC) with electrochemical detection (ECD).

4.2.8 Statistical analysis

Statistical analysis was performed using Prism (v5.0; GraphPad Software, San Diego, CA). Data was presented as the means +/- standard error of the mean (SEM) unless otherwise noted; $P < 0.05$ was considered significant. Experimental values from each mean were analyzed with a ROUT (alpha = 0.05) test to identify and exclude significant outliers. Differences between the viral and the control group were analyzed using an unpaired t-test or repeated measures two-way ANOVA and Šidák's correction for multiple comparisons as described in figure legends.

4.3 Results

4.3.1 Systemic WEEV causes deficits in motor coordination and grip strength

Similar to our previous aim, we performed serial weights at each time point to monitor their overall health status in addition to frequent cage-side observations. The weight curve remained linear in both groups until 21 dpi, when infected groups trended downwards on average while control groups continued to gain weight as expected (Figure 4-2 A). This weight loss appeared to partially recover by 42 dpi, and no single mouse lost more than 5% of their body weight throughout the study. The pole test was used as a measure of motor coordination, a symptom that PD patients often struggle with. Infected mice descended the pole more quickly on average than control mice by 21 dpi, and statistical significance was achieved by 42 dpi (Figure 4-2 B, $p=0.0251$). Grip strength testing is also an excellent indicator of neuropathology, as the

severity of PD is strongly correlated with decreases in grip strength. Average forelimb grip strength gradually decreased in both infected and control mice; however, infected mice exhibited a statistically significant decrease in forelimb grip strength at 42 dpi compared to the control group (Figure 4-2 C, $p=0.0138$). Fixed effects analysis revealed statistical significance of dpi ($p<0.0001$) and PFU ($p=0.0112$) on forelimb grip strength. Average forelimb and hindlimb grip strength was more variable across time points; however, there was a statistically significant decrease in grip strength at 42 dpi (Figure 4-2 D, $p=0.0251$). Fixed effects analysis revealed statistical significance of dpi ($p<0.0001$) and dpi and PFU ($p=0.0228$) on average forelimb and hindlimb grip strength. All mice in this study reached their endpoint without experiencing morbidity or mortality.

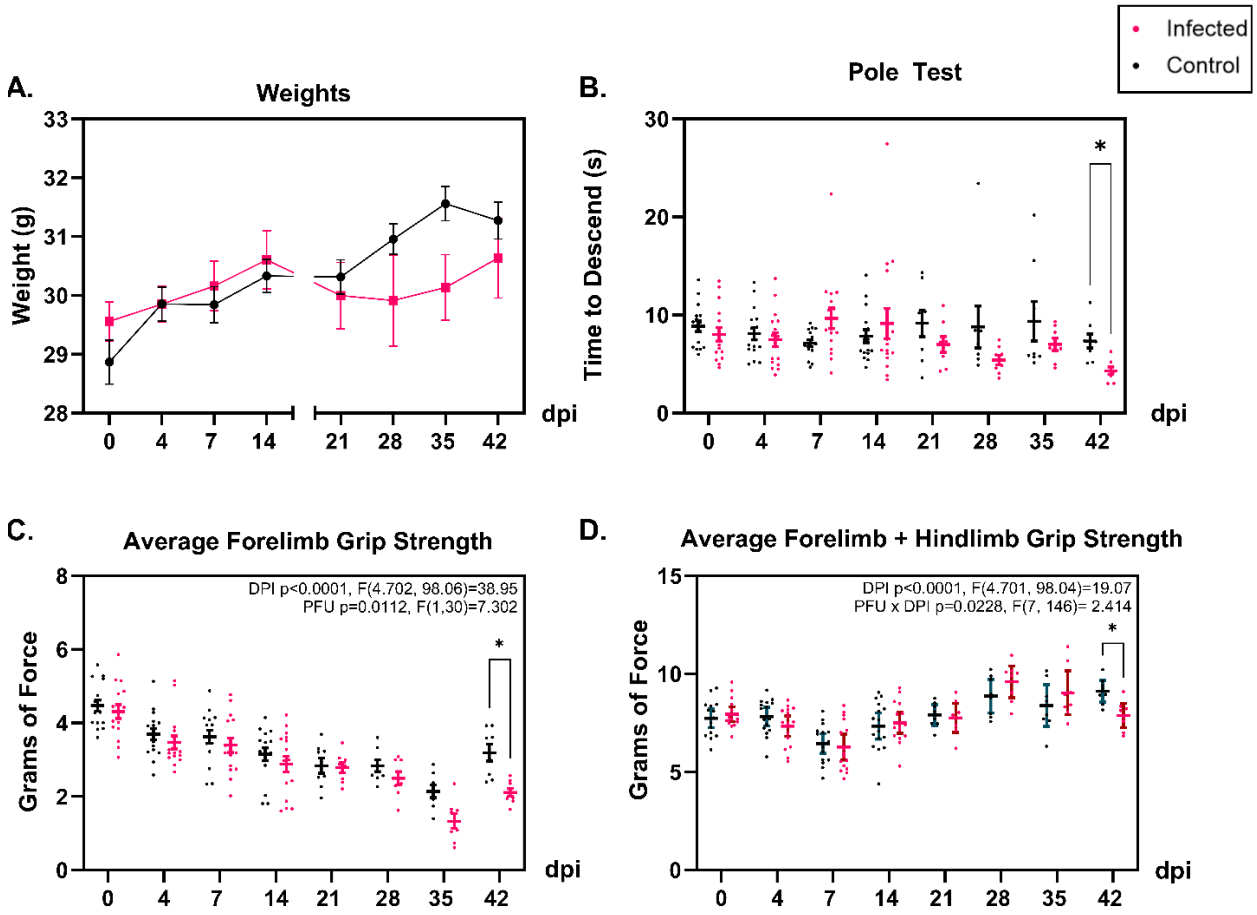

Figure 4-2: Behavioral and physiological changes in mice. Footpad inoculation with recombinant WEEV induces mild weight loss from 21 to 42 dpi (A) after loss of half the mice indicated by the break in the x-axis, and behavioral changes by 42 dpi involving motor coordination as seen in the pole test (B) and grip strength as seen in both the forelimbs (C) and forelimbs and hindlimbs (D). Statistical analysis was performed using Two-Way ANOVA, multiple pairwise comparisons, displayed in mean +/- SEM (n=32, *p<0.05).

4.3.2 Footpad inoculation of WEEV resulted in consistent brain titers

Plaque assays were used in this study to verify the amount of WEEV in the brains of mice as a verification of CNS infection. As expected, all control mice had no plaques (Table 4-1). Representative images of the plaques counted in the assay are provided in Figure 4-3 A and B. While some of the control mouse plates showed scratches on the surface and degradation of the crystal violet dye due to a delay between counting and imaging, a distinct morphological difference

is seen in the plaques of infected mice. When quantified, the viral titer between time points showed a significantly higher titer at 42 dpi compared to 14 dpi (Figure 4-3 C).

Table 4-1 Viral titer loads quantified via plaque assay

Mouse #	Group	# Plaques	Dilution Factor	Volume (mL)	Titer
1-16	Control	0	0	0	0
17	Infected 14dpi	6	1.00E-01	0.12	5.00E+02
18	Infected 14dpi	5	1.00E-02	0.12	4.17E+03
19	Infected 14dpi	4	1.00E-02	0.12	3.33E+03
20	Infected 14dpi	7	1.00E-01	0.12	5.83E+02
21	Infected 42dpi	6	1.00E-03	0.12	5.00E+04
22	Infected 42dpi	5	1.00E-03	0.12	4.17E+04
23	Infected 42dpi	2	1.00E-02	0.12	1.67E+03
24	Infected 42dpi	3	1.00E-03	0.12	2.50E+04
25	Infected 42dpi	2	1.00E-03	0.12	1.67E+04
26	Infected 42dpi	1	1.00E-03	0.12	8.33E+03
27	Infected 42dpi	5	1.00E-04	0.12	4.17E+05
28	Infected 42dpi	6	1.00E-01	0.12	5.00E+02
29	Infected 14dpi	4	1.00E-02	0.12	3.33E+03
30	Infected 14dpi	2	1.00E-02	0.12	1.67E+03
31	Infected 14dpi	6	1.00E-02	0.12	5.00E+03
32	Infected 14dpi	6	1.00E-04	0.12	5.00E+05

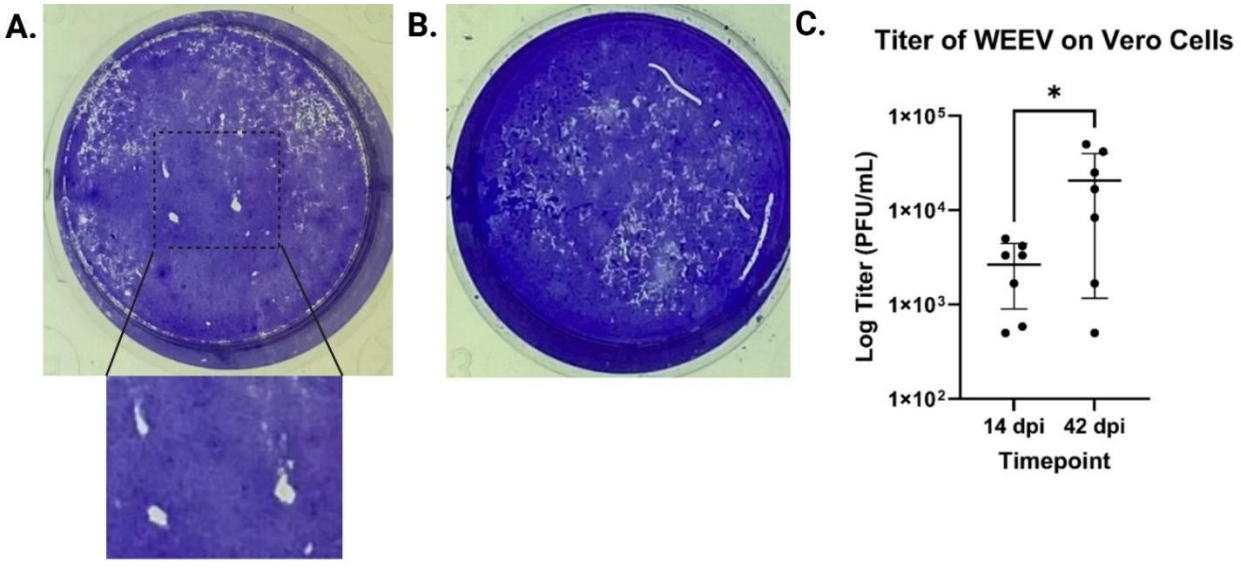

Figure 4-3 Plaque assay representative images and titer. A. One plate from an infected mouse with representative plaques shown. B. One plate from a control mouse with some degradation of

the crystal violet dye and some scratches, but no plaques. C. Titer of WEEV on Vero cells, indicating significance between the two timepoints. Statistical analysis was performed using an unpaired t-test, displayed in mean +/- SEM (n=8, *p<0.05).

4.3.3 Short-term systemic WEEV results in variable neurochemistry quantification

Neurochemistry quantification was used to measure the concentrations of neurotransmitters and their metabolites within the brain to provide insights into brain pathology. The following neurotransmitters were quantified: dopamine (DA), norepinephrine (NE), and serotonin (5-HT), as well as the following metaboltites: 3,4-dihydroxyphenylacetic acid (DOPAC, a metabolite of dopamine), homovanillic acid (HVA, a metabolite of dopamine), 3-Methoxytyramine (3-MT, a metabolite of dopamine), and 5-Hydroxyindoleacetic Acid (5-HIAA, a metabolite of serotonin). A DOPAC/DA ratio is performed to assess the rate of dopamine metabolism. While there is a visually noticeable increase in DOPAC, dopamine, and 3-MT at 14 dpi in infected mice compared to control mice, these changes were not statistically significant ($p=0.4157$, $p=0.3539$, and $p=0.4467$, respectively). No neurotransmitters or their metabolites showed a statistically significant change between infected and control mice at any time point.

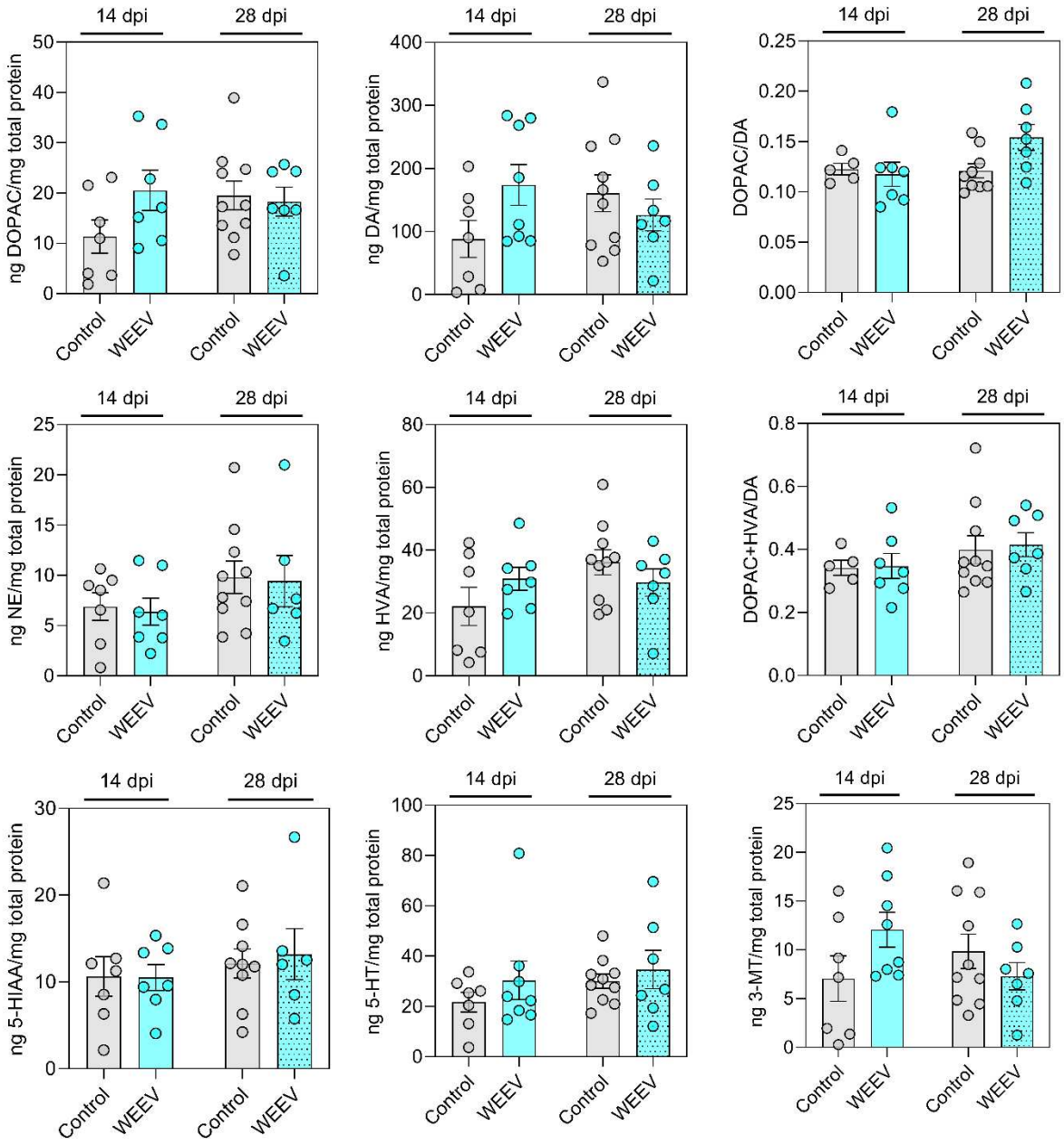

Figure 4-4 Neurochemistry quantification of DOPAC (3,4-dihydroxyphenylacetic acid), DA (dopamine), DOPAC/DA ratio, NE (norepinephrine), HVA (homovanillic acid), DOPAC + HVA, 5-HIAA (5-hydroxyindoleacetic acid), 5-HT (serotonin), and 3-MT (3-Methoxytyramine).

4.4 Discussion

Our previous study established a histopathologic parkinsonian phenotype, but behavioral characteristics could not be clearly elucidated. We hypothesized that a grip strength meter would

result in clearer results compared to the hang test, and that wrapping the pole would provide better traction for the mice. Finally, our previous study showed mortality in relation to isoflurane anesthesia. We hypothesized that this was due to increased sensitivity to anesthesia secondary to viral CNS infection. In the current study, anesthesia was not utilized. Mice were infected with 2 x 10^5 PFU of WEEV via left hind footpad injection and compared to control mice at various days post-infection (dpi).

This study demonstrates that exposure to a selected alphavirus (WEEV) results in the development of a neurodegenerative behavioral phenotype associated with a parkinsonian syndrome in mice. Although infected mice displayed some mild weight changes, mice did not develop changes in their general health related to WEEV, such as lethargy, increased respiratory rate, or hunched posture. An absence of direct lethality and the development of clinical signs that could potentially require euthanasia for welfare purposes creates an optimal animal model for studying disease pathology and therapeutics. In this study, we did not use isoflurane anesthesia associated with the IVIS camera system. Since we did not see any clinical signs of infection requiring euthanasia as seen in pilot 2, this further supports our hypothesis that systemic WEEV infection causes sensitivity to and difficulty recovering from anesthesia.

The pole test and grip strength meter were used in this study to establish the behavioral phenotype of infected mice. There was some variability in the results of both of these tests at earlier time points. Mice did, however, exhibit significant behavioral deficits involving motor coordination and grip strength by 42 dpi, both of which mimic the debilitating functional aspects of PD in humans. One limitation of the pole test is that it is nonspecific for neurodegeneration, as descending a pole is influenced by several aspects of motor function. A multitude of brain and bodily regions are involved in descending the pole, which may contribute to variation between

subjects. Another limitation of behavioral testing in general is subject compliance, which may increase this variability. While more sensitive to motor dysfunction in mice than the pole test, some mice in the control group showed a gradual decrease in grip strength, particularly in the forelimb trials. During later trials, we noted an increasing unwillingness of some control mice to grip onto the wire bar. Therefore, multiple trials per animal were required to generate reliable data. This difficulty in obtaining subject compliance may have caused a gradual decrease in grip strength over time. However, a subsequent decrease seen in infected mice and statistical significance achieved at 42 dpi still indicates a distinct behavioral phenotype. Overall, significant changes to both motor coordination and grip strength on 42 dpi in infected mice compared to control mice indicate that their motor functioning is being altered by the virus.

Interestingly, the neurochemistry quantification revealed no significant changes to dopamine, serotonin, or norepinephrine concentrations or their metabolites in the striata of infected mice compared to control mice, despite a quantifiable neuronal decrease. Confounding variables may have occurred to affect these results, such as inclusion of extraneous tissues other than the striatum, variations in temperature control during shipping, or deviations in the sample preparation and analysis process. In addition, the relationship between neuronal counts and neurochemistry is complex and may not always be linear. A decrease in neuronal density might affect dopamine and other neurochemical counts in unexpected ways due to effects on neural circuit organization and activity. For example, the brain may employ compensatory mechanisms to maintain stable dopamine concentrations despite a decreased dopaminergic neuronal count by altering its reuptake or increasing biosynthesis in remaining neurons [135]. These endogenous mechanisms have been observed in early PD patients and therefore may play a role in the neurochemical results of this short-term study [135]. Extending the time points of infected mice

may result in different neurochemical concentrations as neurons continue to degenerate and compensatory mechanisms become more strained.

In conclusion, systemic WEEV infection induced physiologic and behavioral changes in our mice without incapacitating them, making this a suitable animal model for the study of Parkinson's disease. The previous study demonstrated a clear histopathological phenotype in both the striatum and SNpc. One inherent limitation of this model is the biosafety requirement of an ABSL-3 space. Another limitation is that this model may exhibit sensitivity to isoflurane anesthesia and therefore, may not be suitable for studies requiring anesthesia without further exploration of this mechanism or modifications to the anesthetic technique.

CHAPTER 5 – CONCLUSIONS AND FUTURE DIRECTIONS

This research aimed to characterize a novel mouse model for the study of Parkinson's disease through systemic infection with Western equine encephalitis virus (WEEV) to address the deficiencies of the intranasal inoculation model and further our understanding of the footpad inoculation model.

Firstly, this study expanded upon past studies that investigated the route of entry of WEEV into the CNS by establishing the fundamental behavioral and histopathological changes associated with this infection. To do this, a dose escalation study was conducted to determine the tolerability and preliminary effects of various doses of footpad inoculation of the virus on the mouse. It was determined that the 2×10^5 PFU dose was the most effective at producing neuronal loss in the substantia nigra and striatum. This dose was also generally tolerated by the mice, with the caveat of decreased tolerability to recovering from prolonged anesthesia under isoflurane.

Next, this dose was given to a higher number of mice to confidently establish effects on key brain regions as well as characteristic behavioral changes in infected mice. In this study, a grip strength meter was utilized to more accurately determine grip strength to address variability with the inverted grid test. In addition, anesthesia was not utilized, and all mice reached their study endpoints, further proving that infected mice in the dose escalation studies had decreased tolerability to prolonged anesthesia under isoflurane. One potential future direction would be to explore this mechanism further. Regardless, neuronal loss massively impacted both the substantia nigra and striatum, critical brain regions in the development of PD.

This systemic infection model aligns more closely with the symptomology and pathology of idiopathic PD in humans compared to the intranasal model. Some limitations of this model include an ABSL-3 requirement and sensitivity to isoflurane anesthesia. In addition, the binary usage of only male mice in the characterization study excludes potential differences in behavioral and histopathologic outcomes in female mice. However, future studies can utilize this model to test novel PD therapeutics, including those targeting symptomatic motor relief and those aiming to reduce neurodegeneration, for both safety and efficacy. As novel disease-modifying treatments continue to emerge beyond symptom management, it is critical to have a suitable rodent model to study potential side effects and benefits before progressing to higher-level animal models, such as primates, before ultimately proceeding to clinical trials in humans. While other animal models of PD exist, the ability to recapitulate the disease process in different ways can help us better understand the pathogenesis of the disease and point towards novel treatments.

Finally, a more immediate future direction of this animal model is to combine systemic infection with WEEV with another prominent risk factor of PD. In particular, an environmental toxin such as rotenone or manganese can be co-administered with systemic WEEV to more completely recapitulate the natural disease process in idiopathic PD in humans. This is based on the understanding that exposure to multiple risk factors over a person's lifespan contributes to PD. Therefore, combining risk factors into an animal model may deepen our knowledge of disease pathogenesis and allow for an even more representative animal model for future studies.

REFERENCES

[1] M. T. Hayes, "Parkinson's Disease and Parkinsonism," *American Journal of Medicine*, vol. 132, no. 7, pp. 802–807, Jul. 2019, doi: 10.1016/j.amjmed.2019.03.001.

[2] "Parkinson's disease: Challenges, progress, and promise," NIH National Institute of Neurological Disorders and stroke. Accessed: May 24, 2025. [Online]. Available: https://www.ninds.nih.gov/current-research/focus-disorders/parkinsons-disease-research/parkinsons-disease-challenges-progress-and-promise

[3] W. Yang *et al.*, "Current and projected future economic burden of Parkinson's disease in the U.S.," *NPJ Parkinsons Dis*, vol. 6, no. 1, Dec. 2020, doi: 10.1038/s41531-020-0117-1.

[4] A. H. V Schapira, "Molecular and clinical pathways to neuroprotection of dopaminergic drugs in Parkinson disease," *Neurology*, vol. 72(Suppl 2), pp. S44–S50, Feb. 2009, [Online]. Available: https://www.neurology.org

[5] M. G. Tansey and M. S. Goldberg, "Neuroinflammation in Parkinson's disease: Its role in neuronal death and implications for therapeutic intervention," *Neurobiol Dis*, vol. 37, no. 3, pp. 510–518, Mar. 2010, doi: 10.1016/j.nbd.2009.11.004.

[6] M. J. Armstrong and M. S. Okun, "Diagnosis and Treatment of Parkinson Disease: A Review," Feb. 11, 2020, *American Medical Association*. doi: 10.1001/jama.2019.22360.

[7] V. Leta *et al.*, "Viruses, parkinsonism and Parkinson's disease: the past, present and future," *J Neural Transm*, vol. 129, no. 9, pp. 1119–1132, Sep. 2022, doi: 10.1007/s00702-022-02536-y.

[8] R. J. Smeyne, A. J. Noyce, M. Byrne, R. Savica, and C. Marras, "Infection and risk of Parkinson's disease," 2021, *IOS Press BV*. doi: 10.3233/JPD-202279.

[9] J. Henry, R. J. Smeyne, H. Jang, B. Miller, and M. S. Okun, "Parkinsonism and neurological manifestations of influenza throughout the 20th and 21st centuries," *Parkinsonism Relat Disord*, vol. 16, no. 9, pp. 566–571, Nov. 2010, doi: 10.1016/j.parkreldis.2010.06.012.

[10] B. A. Cunha, "Influenza: historical aspects of epidemics and pandemics," *Infect Dis Clin North Am*, vol. 18, no. 1, pp. 141–155, Mar. 2004.

[11] C. M. Bantle, A. T. Phillips, R. J. Smeyne, S. M. Rocha, K. E. Olson, and R. B. Tjalkens, "Infection with mosquito-borne alphavirus induces selective loss of dopaminergic neurons, neuroinflammation and widespread protein aggregation," *NPJ Parkinsons Dis*, vol. 5, no. 1, Dec. 2019, doi: 10.1038/s41531-019-0090-8.

[12] C. M. Bantle *et al.*, "Astrocyte inflammatory signaling mediates α-synuclein aggregation and dopaminergic neuronal loss following viral encephalitis," *Exp Neurol*, vol. 346, Dec. 2021, doi: 10.1016/j.expneurol.2021.113845.

[13] A. T. Phillips *et al.*, "Entry Sites of Venezuelan and Western Equine Encephalitis Viruses in the Mouse Central Nervous System following Peripheral Infection," *J Virol*, vol. 90, no. 12, pp. 5785–5796, Jun. 2016, doi: 10.1128/jvi.03219-15.

[14] V. L. Feigin *et al.*, "Global, regional, and national burden of neurological disorders, 1990–2016: a systematic analysis for the Global Burden of Disease Study 2016," *Lancet Neurol*, vol. 18, no. 5, pp. 459–480, May 2019, doi: 10.1016/S1474-4422(18)30499-X.

[15] E. R. Dorsey, T. Sherer, M. S. Okun, and B. R. Bloemd, "The emerging evidence of the Parkinson pandemic," 2018, *IOS Press*. doi: 10.3233/JPD-181474.

[16] Geneva: World Health Organization, "Parkinson disease: A public health approach. Technical brief," 2022.

[17] 118th Congress, *Public Law 118-66 "Part W - Parkinson's and Related Disorders."* 2024.

[18] J. Parkinson, "An Essay on the Shaking Palsy," *J Neuropsychiatry Clin Neurosci*, vol. 14, no. 2, 2002.

[19] F. Xing, L. Marsili, and D. D. Truong, "Parkinsonism in viral, paraneoplastic, and autoimmune diseases," *J Neurol Sci*, vol. 433, Feb. 2022, doi: 10.1016/j.jns.2021.120014.

[20] A. A. Moustafa *et al.*, "Motor symptoms in Parkinson's disease: A unified framework," Sep. 01, 2016, *Elsevier Ltd*. doi: 10.1016/j.neubiorev.2016.07.010.

[21] B. R. Bloem, Y. A. M. Grimbergen, M. Cramer, M. Willemsen, and A. H. Zwinderman, "Prospective assessment of falls in Parkinson's disease," *J Neurol*, vol. 248, pp. 950–958, 2001.

[22] S. S. Paul, C. Sherrington, C. G. Canning, V. S. C. Fung, J. C. T. Close, and S. R. Lord, "The relative contribution of physical and cognitive fall risk factors in people with Parkinson's disease: A large prospective cohort study," *Neurorehabil Neural Repair*, vol. 28, no. 3, pp. 282–290, Mar. 2014, doi: 10.1177/1545968313508470.

[23] R. W. Walker, A. Chaplin, R. L. Hancock, R. Rutherford, and W. K. Gray, "Hip fractures in people with idiopathic Parkinson's disease: Incidence and outcomes," *Movement Disorders*, vol. 28, no. 3, pp. 334–340, Mar. 2013, doi: 10.1002/mds.25297.

[24] W. A. den HARTOG JAGER and J. BETHLEM, "The distribution of Lewy bodies in the central and autonomic nervous systems in idiopathic paralysis agitans," *J Neurol Neurosurg Psychiatry*, vol. 23, pp. 283–290, Nov. 1960, doi: 10.1136/jnnp.23.4.283.

[25] M. J. Eadie and J. H. Tyrer, "Alimentary Disorder in Parkinsonism," *Australas Ann Med*, vol. 14, pp. 13–22, 1965, doi: 10.1111/imj.1965.14.1.13.

[26] M. J. Eadie and J. H. Tyrer, "Radiological Abnormalities of the Upper Part of the Alimentary Tract in Parkinsonism," *Australas Ann Med*, vol. 14, pp. 23–27, 1965, doi: 10.1111/imj.1965.14.1.23.

[27] M. Bushmann, S. M. Dobmeyer, L. Leeker, and J. S. Perlmutter, “Swallowing abnormalities and their response to treatment in Parkinson’s disease,” *Neurology*, vol. 39, pp. 1309–1314, Oct. 1989, [Online]. Available: https://www.neurology.org

[28] L. Edwards, E. M. M. Quigley, R. Hofman, and R. F. Pfeiffer, “Gastrointestinal symptoms in parkinson disease: 18-month follow-up study,” *Movement Disorders*, vol. 8, no. 1, pp. 83–86, 1993, doi: 10.1002/mds.870080115.

[29] M. Lubomski, R. L. Davis, and C. M. Sue, “Gastrointestinal dysfunction in Parkinson’s disease,” *J Neurol*, vol. 267, no. 5, pp. 1377–1388, May 2020, doi: 10.1007/s00415-020-09723-5.

[30] M. Lubomski, R. L. Rushworth, and S. Tisch, “Hospitalisation and comorbidities in Parkinson’s disease: A large Australian retrospective study,” *J Neurol Neurosurg Psychiatry*, vol. 86, no. 3, pp. 324–329, Mar. 2015, doi: 10.1136/jnnp-2014-307822.

[31] T. Warnecke, K. H. Schäfer, I. Claus, K. Del Tredici, and W. H. Jost, “Gastrointestinal involvement in Parkinson’s disease: pathophysiology, diagnosis, and management,” Dec. 01, 2022, *Nature Research*. doi: 10.1038/s41531-022-00295-x.

[32] R. D. Abbott *et al.*, “Frequency of bowel movements and the future risk of Parkinson’s disease,” *Neurology*, vol. 57, pp. 456–462, Feb. 2001, [Online]. Available: https://www.neurology.org

[33] M. G. Stokholm, E. H. Danielsen, S. J. Hamilton-Dutoit, and P. Borghammer, “Pathological α-synuclein in gastrointestinal tissues from prodromal Parkinson disease patients,” *Ann Neurol*, vol. 79, no. 6, pp. 940–949, Jun. 2016, doi: 10.1002/ana.24648.

[34] D. Aarsland *et al.*, “Range of neuropsychiatric disturbances in patients with Parkinson’s disease,” *J Neurol Neurosurg Psychiatry*, vol. 67, pp. 492–496, Apr. 1999.

[35] J. W. Han *et al.*, “Psychiatric manifestation in patients with parkinson’s disease,” *J Korean Med Sci*, vol. 33, no. 47, 2018, doi: 10.3346/jkms.2018.33.e300.

[36] S. Nazem *et al.*, “Suicidal and death ideation in Parkinson’s disease,” *Movement Disorders*, vol. 23, no. 11, pp. 1573–1579, Aug. 2008, doi: 10.1002/mds.22130.

[37] V. S. Kostić *et al.*, “Suicide and suicidal ideation in Parkinson’s disease,” *J Neurol Sci*, vol. 289, no. 1–2, pp. 40–43, Feb. 2010, doi: 10.1016/j.jns.2009.08.016.

[38] C. Klein and A. Westenberger, “Genetics of Parkinson’s disease,” *Cold Spring Harb Perspect Med*, vol. 2, no. 1, 2012, doi: 10.1101/cshperspect.a008888.

[39] B. Thomas and M. Flint Beal, “Parkinson’s disease,” *Hum Mol Genet*, vol. 16, no. R2, pp. R183–R194, Oct. 2007, doi: 10.1093/hmg/ddm159.

[40] S. M. Goldman *et al.*, “Concordance for Parkinson’s disease in twins: A 20-year update,” *Ann Neurol*, vol. 85, no. 4, pp. 600–605, Apr. 2019, doi: 10.1002/ana.25441.

[41] C. M. Tanner *et al.*, “Rotenone, paraquat, and Parkinson’s disease,” *Environ Health Perspect*, vol. 119, no. 6, pp. 866–872, Jun. 2011, doi: 10.1289/ehp.1002839.

[42] A. D. Van Laar *et al.*, “Transient exposure to rotenone causes degeneration and progressive parkinsonian motor deficits, neuroinflammation, and synucleinopathy,” *NPJ Parkinsons Dis*, vol. 9, no. 1, Dec. 2023, doi: 10.1038/s41531-023-00561-6.

[43] M. A. Kioumourtzoglou *et al.*, “Long-term PM2.5 exposure and neurological hospital admissions in the northeastern United States,” *Environ Health Perspect*, vol. 124, no. 1, pp. 23–29, Jan. 2016, doi: 10.1289/ehp.1408973.

[44] P. K. Crane *et al.*, “Association of traumatic brain injury with late-life neurodegenerative conditions and Neuropathologic findings,” *JAMA Neurol*, vol. 73, no. 9, pp. 1062–1069, Sep. 2016, doi: 10.1001/jamaneurol.2016.1948.

[45] J. Gorell, C. Johnson, B. Rybicki, E. Peterson, R. Richardson, and J. M. Gorell, “The risk of Parkinson’s disease with exposure to pesticides, farming, well water, and rural living,” *Neurology*, vol. 50, pp. 1346–1350, May 1998, [Online]. Available: https://www.neurology.org

[46] W. W. Dlamini, G. Nelson, S. S. Nielsen, and B. A. Racette, “Manganese exposure, parkinsonian signs, and quality of life in South African mine workers,” *Am J Ind Med*, vol. 63, no. 1, pp. 36–43, Jan. 2020, doi: 10.1002/ajim.23060.

[47] D. Cabezudo, V. Baekelandt, and E. Lobbestael, “Multiple-Hit Hypothesis in Parkinson’s Disease: LRRK2 and Inflammation,” *Front Neurosci*, vol. 14, no. 376, Apr. 2020, doi: 10.3389/fnins.2020.00376.

[48] D. A. Kalashnikov, J. L. Schnell, J. T. Abatzoglou, D. L. Swain, and D. Singh, “Increasing co-occurrence of fine particulate matter and ground-level ozone extremes in the western United States,” *Sci. Adv*, vol. 8, Jan. 2022, [Online]. Available: https://www.science.org

[49] Y. Smith and J. G. Masilamoni, “Substantia Nigra,” in *Encyclopedia of Movement Disorders*, Katie Kompoliti and Leo Verhagen Metman, Eds., Elsevier, 2010, pp. 189–192. doi: 10.1016/B978-0-12-374105-9.00288-4.

[50] J. M. Fearnley and A. J. Lees, “Ageing and Parkinson’s disease: substantia nigra regional selectivity,” *Brain*, vol. 114, no. 5, pp. 2283–2301, 1991, doi: 10.1093/brain/114.5.2283.

[51] S. Greffard *et al.*, “Motor Score of the Unified Parkinson Disease Rating Scale as a Good Predictor of Lewy Body–Associated Neuronal Loss in the Substantia Nigra,” *Arch Neurol*, vol. 63, no. 4, p. 584, Apr. 2006, doi: 10.1001/archneur.63.4.584.

[52] A. Kouli, K. M. Torsney, and W.-L. Kuan, “Parkinson’s Disease: Etiology, Neuropathology, and Pathogenesis,” in *Parkinson’s Disease: Pathogenesis and Clinical Aspects*, Thomas B. Stoker and Julia C. Greenland, Eds., Brisbane: Codon Publications, 2018, pp. 3–26. doi: 10.15586/codonpublications.parkinsonsdisease.2018.ch1.

[53] P. Calabresi, A. Mechelli, G. Natale, L. Volpicelli-Daley, G. Di Lazzaro, and V. Ghiglieri, “Alpha-synuclein in Parkinson’s disease and other synucleinopathies: from overt neurodegeneration back to early synaptic dysfunction,” *Cell Death Dis*, vol. 14, no. 3, Mar. 2023, doi: 10.1038/s41419-023-05672-9.

[54] E. L. Beatman *et al.*, “Alpha-Synuclein Expression Restricts RNA Viral Infections in the Brain,” *J Virol*, vol. 90, no. 6, pp. 2767–2782, Mar. 2016, doi: 10.1128/JVI.02949-15.

[55] D. C. Wu *et al.*, “Blockade of Microglial Activation Is Neuroprotective in the 1-Methyl-4-Phenyl-1,2,3,6-Tetrahydropyridine Mouse Model of Parkinson Disease,” 2002.

[56] Y. He, S. Appel, and W. Le, “Minocycline inhibits microglial activation and protects nigral cells after 6-hydroxydopamine injection into mouse striatum,” 2001. [Online]. Available: www.elsevier.com/locate/bres

[57] C. H. Williams-Gray *et al.*, “Serum immune markers and disease progression in an incident Parkinson’s disease cohort (ICICLE-PD),” *Movement Disorders*, vol. 31, no. 7, pp. 995–1003, Jul. 2016, doi: 10.1002/mds.26563.

[58] L. F. Gonzalez-Cuyar *et al.*, “Quantitative neuropathology associated with chronic manganese exposure in South African mine workers,” *Neurotoxicology*, vol. 45, pp. 260–266, Dec. 2014, doi: 10.1016/j.neuro.2013.12.008.

[59] D. Scieszka *et al.*, “Biomass smoke inhalation promotes neuroinflammatory and metabolomic temporal changes in the hippocampus of female mice,” *J Neuroinflammation*, vol. 20, no. 1, p. 192, Aug. 2023, doi: 10.1186/s12974-023-02874-y.

[60] A. Adamu, S. Li, F. Gao, and G. Xue, “The role of neuroinflammation in neurodegenerative diseases: current understanding and future therapeutic targets,” *Front Aging Neurosci*, vol. 16, Apr. 2024, doi: 10.3389/fnagi.2024.1347987.

[61] L. Iovino, M. E. Tremblay, and L. Civiero, “Glutamate-induced excitotoxicity in Parkinson’s disease: The role of glial cells,” *J Pharmacol Sci*, vol. 144, no. 3, pp. 151–164, Nov. 2020, doi: 10.1016/j.jphs.2020.07.011.

[62] N. K. Bhol *et al.*, “The interplay between cytokines, inflammation, and antioxidants: mechanistic insights and therapeutic potentials of various antioxidants and anti-cytokine compounds,” *Biomedicine & Pharmacotherapy*, vol. 178, p. 117177, Sep. 2024, doi: 10.1016/j.biopha.2024.117177.

[63] J. Yang *et al.*, “New insight into neurological degeneration: Inflammatory cytokines and blood–brain barrier,” *Front Mol Neurosci*, vol. 15, Oct. 2022, doi: 10.3389/fnmol.2022.1013933.

[64] I. Zahoor, A. Shafi, and E. Haq, “Pharmacological Treatment of Parkinson’s Disease,” in *Parkinson’s Disease: Pathogenesis and Clinical Aspects*, T. Stoker and Greenland JC, Eds., Brisbane: Codon Publications, 2018, ch. 7, pp. 129–144. doi: 10.15586/codonpublications.parkinsonsdisease.2018.ch7.

[65] L. R. Lampariello, A. Cortelazzo, R. Guerranti, C. Sticozzi, and G. Valacchi, “The Magic Velvet Bean of Mucuna pruriens,” 2011.

[66] W. J. Weiner, “Initial Treatment of Parkinson Disease,” *Arch Neurol*, vol. 61, no. 12, pp. 1966–1969, Dec. 2004, doi: 10.1001/archneur.61.12.1966.

[67] C. Trenkwalder, M. Kuoppamäki, M. Vahteristo, T. Müller, and J. Ellmén, “Increased dose of carbidopa with levodopa and entacapone improves ‘off’ time in a randomized trial,” *Neurology*, vol. 92, no. 13, pp. E1487–E1496, Mar. 2019, doi: 10.1212/WNL.0000000000007173.

[68] W. H. Oertel, “Recent advances in treating Parkinson’s disease,” 2017, *Faculty of 1000 Ltd*. doi: 10.12688/f1000research.10100.1.

[69] D. W. Brodell, N. T. Stanford, C. E. Jacobson, P. Schmidt, and M. S. Okun, “Carbidopa/levodopa dose elevation and safety concerns in Parkinson’s patients: a cross-sectional and cohort design”, doi: 10.1136/bmjopen-2012.

[70] P. Brundin, K. D. Dave, and J. H. Kordower, “Therapeutic approaches to target alpha-synuclein pathology,” Dec. 01, 2017, *Academic Press Inc.* doi: 10.1016/j.expneurol.2017.10.003.

[71] T. B. Stoker, K. M. Torsney, and R. A. Barker, “Emerging treatment approaches for Parkinson’s disease,” Oct. 08, 2018, *Frontiers Media S.A.* doi: 10.3389/fnins.2018.00693.

[72] J. A. Vilensky, S. Gilman, and S. McCall, “A historical analysis of the relationship between encephalitis lethargica and postencephalitic parkinsonism: A complex rather than a direct relationship,” Jul. 15, 2010, *John Wiley and Sons Inc.* doi: 10.1002/mds.22908.

[73] L. A. Hoffman and J. A. Vilensky, “Encephalitis lethargica: 100 years after the epidemic,” *Brain*, vol. 140, no. 8, pp. 2246–2251, Aug. 2017, doi: 10.1093/brain/awx177.

[74] T. Haraguchi *et al.*, “An autopsy case of postencephalitic parkinsonism of von Economo type: Some new observations concerning neurofibrillary tangles and astrocytic tangles,” *Neuropathology*, vol. 20, no. 2, pp. 143–148, 2000, doi: 10.1046/j.1440-1789.2000.00287.x.

[75] J. A. Vilensky, C. G. Goetz, and S. Gilman, “Movement disorders associated with encephalitis lethargica: A video compilation,” Jan. 2006. doi: 10.1002/mds.20722.

[76] T. P. Johnson and A. Nath, “Neurological syndromes driven by postinfectious processes or unrecognized persistent infections,” Jun. 01, 2018, *Lippincott Williams and Wilkins*. doi: 10.1097/WCO.0000000000000553.

[77] D. S. Mysiris *et al.*, “Post-COVID-19 Parkinsonism and Parkinson’s Disease Pathogenesis: The Exosomal Cargo Hypothesis,” Sep. 01, 2022, *MDPI*. doi: 10.3390/ijms23179739.

[78] S. Sadasivan, M. Zanin, K. O’Brien, S. Schultz-Cherry, and R. J. Smeyne, “Induction of microglia activation after infection with the non-neurotropic A/CA/04/2009 H1N1 influenza virus,” *PLoS One*, vol. 10, no. 4, Apr. 2015, doi: 10.1371/journal.pone.0124047.

[79] L. Jiao *et al.*, “The olfactory route is a potential way for SARS-CoV-2 to invade the central nervous system of rhesus monkeys,” *Signal Transduct Target Ther*, vol. 6, no. 1, Dec. 2021, doi: 10.1038/s41392-021-00591-7.

[80] M. D. Cain *et al.*, “Virus entry and replication in the brain precedes blood-brain barrier disruption during intranasal alphavirus infection,” *J Neuroimmunol*, vol. 308, pp. 118–130, Jul. 2017, doi: 10.1016/j.jneuroim.2017.04.008.

[81] H. Qiao *et al.*, “Microglia innate immune response contributes to the antiviral defense and blood–CSF barrier function in human choroid plexus organoids during HSV-1 infection,” *J Med Virol*, vol. 95, no. 2, Feb. 2023, doi: 10.1002/jmv.28472.

[82] D. Sulzer *et al.*, “COVID-19 and possible links with Parkinson’s disease and parkinsonism: from bench to bedside,” Dec. 01, 2020, *Nature Research*. doi: 10.1038/s41531-020-00123-0.

[83] C. M. Bosanko *et al.*, “West Nile Virus Encephalitis Involving the Substantia Nigra,” *Arch Neurol*, vol. 60, no. 10, p. 1448, Oct. 2003, doi: 10.1001/archneur.60.10.1448.

[84] B. H. Falkenburger, T. Saridaki, and E. Dinter, “Cellular models for Parkinson’s disease,” Oct. 01, 2016, *Blackwell Publishing Ltd*. doi: 10.1111/jnc.13618.

[85] M. Sedelis, R. K. W. Schwarting, and J. P. Huston, “Behavioral phenotyping of the MPTP mouse model of Parkinson’s disease,” 2001. [Online]. Available: www.elsevier.com/locate/bbr

[86] E. A. Konnova and M. Swanberg, “Animal Models of Parkinson’s Disease,” in *Parkinson’s Disease Pathogenesis and Clinical Aspects*, Brisbane: Codon Publications, 2018, ch. 5, pp. 83–106.

[87] N. Pirzada, “The Ethical Dilemma of Non-Human Primate Use in Biomedical Research,” *Voices in Bioethics*, vol. 8, Feb. 2022, doi: 10.52214/vib.v8i.9348.

[88] U. Ungerstedt, “6-Hydroxydopamine-induced degeneration of the nigrostriatal dopamine pathway: the turning syndrome,” *Pharmacol Ther*, vol. 2, no. 1, pp. 37–40, 1976.

[89] C. Latchoumycandane, V. Anantharam, H. Jin, A. Kanthasamy, and A. Kanthasamy, “Dopaminergic neurotoxicant 6-OHDA induces oxidative damage through proteolytic activation of PKCδ in cell culture and animal models of Parkinson’s disease,” *Toxicol Appl Pharmacol*, vol. 256, no. 3, pp. 314–323, Nov. 2011, doi: 10.1016/j.taap.2011.07.021.

[90] T. Hokfelt and U. Ungerstedt, “Specificity of 6-hydroxydopamine induced degeneration of central monoamine neurones: an electron and fluorescence microscopic study with special reference to intracerebral injection on the nigro-striatal dopamine system,” *Brain Res*, vol. 60, pp. 269–297, Mar. 1973.

[91] K. Sakai and D. M. Gash, “Effect of bilateral 6-OHDA lesions of the substantia nigra on locomotor activity in the rat,” *Brain Res*, vol. 633, pp. 144–150, Aug. 1994.

[92] A. Eslamboli *et al.*, “Continuous low-level glial cell line-derived neurotrophic factor delivery using recombinant adeno-associated viral vectors provides neuroprotection and induces behavioral recovery in a primate model of Parkinson’s disease,” *Journal of Neuroscience*, vol. 25, no. 4, pp. 769–777, Feb. 2005, doi: 10.1523/JNEUROSCI.4421-04.2005.

[93] A. Giovanni, B. A. Sieber, R. E. Heikkila, and P. K. Sonsalla, “Studies on species sensitivity to the dopaminergic neurotoxin 1-methyl-4-phenyl-1,2,3,6-tetrahydropyridine. Part 1: Systemic administration.,” *J Pharmacol Exp Ther*, vol. 270, no. 3, pp. 1000–7, Sep. 1994.

[94] S. Przedborski and M. Vila, “MPTP: a review of its mechanisms of neurotoxicity,” *Clin Neurosci Res*, pp. 407–418, Aug. 2001, [Online]. Available: www.elsevier.com/locate/clires

[95] W. Song *et al.*, “Infiltrating peripheral monocyte TREM-1 mediates dopaminergic neuron injury in substantia nigra of Parkinson’s disease model mice,” *Cell Death Dis*, vol. 16, no. 1, p. 18, Dec. 2025, doi: 10.1038/s41419-025-07333-5.

[96] R. K. W. Schwarting, M. Sedelis, K. Hofele, G. W. Auburger, and J. P. Huston, “Strain-dependent recovery of open-field behavior and striatal dopamine deficiency in the mouse MPTP model of Parkinson’s disease,” *Neurotox Res*, vol. 1, no. 1, pp. 41–56, Mar. 1999, doi: 10.1007/BF03033338.

[97] S. H. Fox and J. M. Brotchie, “The MPTP-lesioned non-human primate models of Parkinson’s disease. Past, present, and future,” in *Progress in Brain Reserach*, vol. 184, Anders Björklund and Angela Cenci, Eds., Elsevier, 2010, ch. 7, pp. 133–157. doi: 10.1016/S0079-6123(10)84007-5.

[98] J. R. Cannon, V. Tapias, H. M. Na, A. S. Honick, R. E. Drolet, and J. T. Greenamyre, “A highly reproducible rotenone model of Parkinson’s disease,” *Neurobiol Dis*, vol. 34, no. 2, pp. 279–290, May 2009, doi: 10.1016/j.nbd.2009.01.016.

[99] F. García-García, S. Ponce, R. Brown, V. Cussen, and J. M. Krueger, “Sleep disturbances in the rotenone animal model of Parkinson disease,” *Brain Res*, vol. 1042, no. 2, pp. 160–168, May 2005, doi: 10.1016/j.brainres.2005.02.036.

[100] A. L. McCormack *et al.*, “Environmental risk factors and Parkinson’s disease: Selective degeneration of nigral dopaminergic neurons caused by the herbicide paraquat,” *Neurobiol Dis*, vol. 10, no. 2, pp. 119–127, 2002, doi: 10.1006/nbdi.2002.0507.

[101] Q. Cai, Y. Jin, Z. Jia, and Z. Liu, “Paraquat Induces Lung Injury via miR-199-Mediated SET in a Mouse Model,” *Front Pharmacol*, vol. 13, Apr. 2022, doi: 10.3389/fphar.2022.856441.

[102] J. Donaldson, D. McGregor, and F. LaBella, “Manganese neurotoxicity: a model for free radical mediated neurodegeneration?,” *Can J Physiol Pharmacol*, vol. 60, no. 11, pp. 1398–1405, Nov. 1982, doi: 10.1139/y82-208.

[103] P. J. Kontur and L. D. Fechter, “Brain Regional Manganese Levels and Monoamine Metabolism in Manganese-Treated Neonatal Rats,” *Neurotoxicol Teratol*, vol. 10, pp. 295–303, May 1988.

[104] T. M. Peneder *et al.*, “Chronic exposure to manganese decreases striatal dopamine turnover in human alpha-synuclein transgenic mice,” *Neuroscience*, vol. 180, pp. 280–292, Apr. 2011, doi: 10.1016/j.neuroscience.2011.02.017.

[105] M. R. Avila-Costa, J. L. Ordoñez-Librado, V. Anaya-Martínez, A. L. Gutierrez-Valdez, L. Colín-Barenque, and E. Montiel-Flores, "Manganese inhalation as a Parkinson disease model," *Parkinsons Dis*, vol. 2011, Dec. 2010, doi: 10.4061/2011/612989.

[106] M. Sabbar, C. Delaville, P. De Deurwaerdère, N. Lakhdar-Ghazal, and A. Benazzouz, "Lead-induced atypical Parkinsonism in rats: Behavioral, electrophysiological, and neurochemical evidence for a role of noradrenaline depletion," *Front Neurosci*, vol. 12, no. MAR, Mar. 2018, doi: 10.3389/fnins.2018.00173.

[107] T. Kitada, Y. Tong, C. A. Gautier, and J. Shen, "Absence of nigral degeneration in aged parkin/DJ-1/PINK1 triple knockout mice," *J Neurochem*, vol. 111, no. 3, pp. 696–702, Nov. 2009, doi: 10.1111/j.1471-4159.2009.06350.x.

[108] D. M. Hendrickx *et al.*, "A New Synuclein-Transgenic Mouse Model for Early Parkinson's Reveals Molecular Features of Preclinical Disease," *Mol Neurobiol*, vol. 58, no. 2, pp. 576–602, Feb. 2021, doi: 10.1007/s12035-020-02085-z.

[109] M. Massaro Cenere *et al.*, "Systemic inflammation accelerates neurodegeneration in a rat model of Parkinson's disease overexpressing human alpha synuclein," *NPJ Parkinsons Dis*, vol. 10, no. 1, p. 213, Nov. 2024, doi: 10.1038/s41531-024-00824-w.

[110] A. Van der Perren, C. Van den Haute, and V. Baekelandt, "Viral Vector-Based Models of Parkinson's Disease," in *Behavioral Neurobiology of Huntington's Disease and Parkinson's Disease*, vol. 22, H. Nguyen and M. Cenci, Eds., Berlin: Springer, 2014, pp. 271–301. [Online]. Available: http://www.springer.com/series/7854

[111] A. Ogata, K. Tashiro, S. Nukuzuma, K. Nagashima, and W. W. Hall, "A rat model of Parkinson's disease induced by Japanese encephalitis virus," *J Neurovirol*, vol. 3, no. 2, pp. 141–147, Jan. 1997, doi: 10.3109/13550289709015803.

[112] C. Fongsaran, K. T. Dineley, S. Paessler, and I. E. Cisneros, "VEEV TC-83 Triggers Dysregulation of the Tryptophan–Kynurenine Pathway in the Central Nervous System That Correlates with Cognitive Impairment in Tg2576 Mice," *Pathogens*, vol. 13, no. 5, May 2024, doi: 10.3390/pathogens13050397.

[113] C. H. Calisher, "Medically Important Arboviruses of the United States and Canada," 1994. [Online]. Available: https://journals.asm.org/journal/cmr

[114] R. Whitley and J. Gnann, "Viral encephalitis: familiar infections and emerging pathogens," *The Lancet*, vol. 359, pp. 507–514, Feb. 2002, [Online]. Available: www.thelancet.com

[115] K. E. Steele and N. A. Twenhafel, "Pathology of animal models of alphavirus encephalitis," *Vet Pathol*, vol. 47, no. 5, pp. 790–805, Sep. 2010, doi: 10.1177/0300985810372508.

[116] P. J. Meechan and J. Potts, *Biosafety in microbiological and biomedical laboratories*, 6th ed. Centers for Disease Control and Prevention (U.S.) ; National Institutes of Health (U.S.), 2020.

[117] A. S. Campos *et al.*, "Molecular Epidemiology of Western Equine Encephalitis Virus, South America, 2023–2024," *Emerg Infect Dis*, vol. 30, no. 9, pp. 1834–1840, Sep. 2024, doi: 10.3201/eid3009.240530.

[118] C. H. Calisher, “Medically Important Arboviruses of the United States and Canada,” *Clin Microbiol Rev*, pp. 89–116, Jan. 1994.

[119] B. Rozdilsky, H. E. Robertson, and J. Chorney, “Western Encephalitis: Report of Eight Fatal Cases: Saskatchewan Epidemic, 1965,” *Canad. Med. Ass. J.*, vol. 98, Jan. 1968.

[120] D. W. Mulder, M. Parrott, and M. Thaler, “Sequelae of Western Equine Encephalitis,” *Neurology*, vol. 1, no. 7–8, pp. 318–318, Jul. 1951, doi: 10.1212/WNL.1.7-8.318.

[121] D. R. Schultz, J. S. Barthal, and C. Garrett, “Brief communications Western equine encephalitis with rapid onset of parkinsonism,” 1977. [Online]. Available: https://www.neurology.org

[122] A. L. Phelps *et al.*, “Susceptibility and lethality of western equine encephalitis virus in Balb/c mice when infected by the aerosol route,” *Viruses*, vol. 9, no. 7, Jul. 2017, doi: 10.3390/v9070163.

[123] A. T. Phillips *et al.*, “Bioluminescent Imaging and Histopathologic Characterization of WEEV Neuroinvasion in Outbred CD-1 Mice,” *PLoS One*, vol. 8, no. 1, p. e53462, Jan. 2013, doi: 10.1371/journal.pone.0053462.

[124] K. M. Long and M. Heise, “Safe and Effective Mouse Footpad Inoculation,” in *Mouse Models of Innate Immunity. Methods in Molecular Biology*, vol. 1031, I. C. Allen, Ed., Totowa, NJ: Humana Press, 2013, pp. 97–100. doi: https://doi.org/10.1007/978-1-62703-481-4_12.

[125] K. Matsuura, H. Kabuto, H. Makino, and N. Ogawa, “Pole test is a useful method for evaluating the mouse movement disorder caused by striatal dopamine depletion,” 1997.

[126] A. Mann and M. F. Chesselet, “Techniques for Motor Assessment in Rodents,” in *Movement Disorders: Genetics and Models: Second Edition*, Elsevier Inc., 2015, ch. 8, pp. 139–157. doi: 10.1016/B978-0-12-405195-9.00008-1.

[127] L. M. Stollings, L. J. Jia, P. Tang, H. Dou, B. Lu, and Y. Xu, “Immune modulation by volatile anesthetics,” Aug. 01, 2016, *Lippincott Williams and Wilkins*. doi: 10.1097/ALN.0000000000001195.

[128] Y. M. Lee, B. C. Song, and K. J. Yeum, “Impact of Volatile Anesthetics on Oxidative Stress and Inflammation,” 2015, *Hindawi Publishing Corporation*. doi: 10.1155/2015/242709.

[129] N. Schallner *et al.*, “Isoflurane but Not Sevoflurane or Desflurane Aggravates Injury to Neurons In Vitro and In Vivo via p75NTR-NF-κB Activation,” *Anesth Analg*, vol. 119, no. 6, pp. 1429–1441, Dec. 2014, doi: 10.1213/ANE.0000000000000488.

[130] I. N Krout, A. White, and T. Sampson, “Pole Test Assessment,” Aug. 08, 2024. doi: 10.17504/protocols.io.n92ld8j87v5b/v1.

[131] K. E. Glajch, S. M. Fleming, D. J. Surmeier, and P. Osten, “Sensorimotor assessment of the unilateral 6-hydroxydopamine mouse model of Parkinson’s disease,” *Behavioural Brain Research*, vol. 230, no. 2, pp. 309–316, May 2012, doi: 10.1016/j.bbr.2011.12.007.

[132] M. Sedelis, K. Hofele, and G. Aubuger, “MPTP Susceptibility in the Mouse: Behavioral, Neurochemical, and Histological Analysis of Gender and Strain Differences”.

[133] J. J. Munier *et al.*, “Simultaneous monitoring of mouse grip strength, force profile, and cumulative force profile distinguishes muscle physiology following surgical, pharmacologic and diet interventions,” *Sci Rep*, vol. 12, no. 1, Dec. 2022, doi: 10.1038/s41598-022-20665-y.

[134] C. M. Bantle, A. T. Phillips, R. J. Smeyne, S. M. Rocha, K. E. Olson, and R. B. Tjalkens, “Infection with mosquito-borne alphavirus induces selective loss of dopaminergic neurons, neuroinflammation and widespread protein aggregation,” *NPJ Parkinsons Dis*, vol. 5, no. 1, Dec. 2019, doi: 10.1038/s41531-019-0090-8.

[135] J. Brotchie and C. Fitzer-Attas, “Mechanisms compensating for dopamine loss in early Parkinson disease,” *Neurology*, vol. 72, no. 7_supplement_2, Feb. 2009, doi: 10.1212/WNL.0b013e318198e0e9.